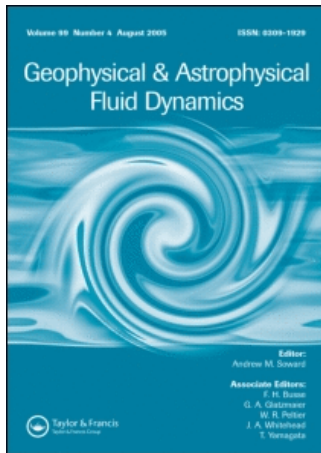


This article was downloaded by:[Observatoire de Paris-Section]
On: 9 October 2007
Access Details: [subscription number 768491691]
Publisher: Taylor & Francis
Informa Ltd Registered in England and Wales Registered Number: 1072954
Registered office: Mortimer House, 37-41 Mortimer Street, London W1T 3JH, UK



Geophysical & Astrophysical Fluid Dynamics

Publication details, including instructions for authors and subscription information:
<http://www.informaworld.com/smpp/title~content=t713642804>

On the magnetic fields generated by experimental dynamos

F. Pétrélis; N. Mordant; S. Fauve

Online Publication Date: 01 June 2007

To cite this Article: Pétrélis, F., Mordant, N. and Fauve, S. (2007) 'On the magnetic fields generated by experimental dynamos', Geophysical & Astrophysical Fluid Dynamics, 101:3, 289 - 323

To link to this article: DOI: 10.1080/03091920701523410

URL: <http://dx.doi.org/10.1080/03091920701523410>

PLEASE SCROLL DOWN FOR ARTICLE

Full terms and conditions of use: <http://www.informaworld.com/terms-and-conditions-of-access.pdf>

This article maybe used for research, teaching and private study purposes. Any substantial or systematic reproduction, re-distribution, re-selling, loan or sub-licensing, systematic supply or distribution in any form to anyone is expressly forbidden.

The publisher does not give any warranty express or implied or make any representation that the contents will be complete or accurate or up to date. The accuracy of any instructions, formulae and drug doses should be independently verified with primary sources. The publisher shall not be liable for any loss, actions, claims, proceedings, demand or costs or damages whatsoever or howsoever caused arising directly or indirectly in connection with or arising out of the use of this material.

On the magnetic fields generated by experimental dynamos

F. PÉTRÉLIS*, N. MORDANT and S. FAUVE

LPS, CNRS UMR 8550, Ecole Normale Supérieure, 24 rue Lhomond,
75005 Paris France

(Received 19 March 2007; in final form 28 May 2007)

We review the results obtained by three successful fluid dynamo experiments and discuss what has been learnt from them about the effect of turbulence on the dynamo threshold and saturation. We then discuss several questions that are still open and propose experiments that could be performed to answer some of them.

Keywords: Dynamo instability; Experimental dynamos; Magnetohydrodynamics; Turbulence

1. Fluid dynamos

It is now believed that magnetic fields of planets and stars are generated by the motion of electrically conducting fluids through the dynamo process. This has been first proposed by Larmor (Larmor 1919) for the magnetic field of the sun. Assuming the existence of an initial perturbation of magnetic field, he observed that “internal motion induces an electric field acting on the moving matter: and if any conducting path around the solar axis happens to be open, an electric current will flow round it, which may in turn increase the inducing magnetic field. In this way it is possible for the internal cyclic motion to act after the manner of the cycle of a self-exciting dynamo, and maintain a permanent magnetic field from insignificant beginnings, at the expense of some of the energy of the internal circulation” (for reviews of the subject, see Moffatt 1978, Zeldovich *et al.* 1983, Roberts 1994).

The minimum set of parameters involved in a fluid dynamo consists of the size of the flow domain, L , the typical fluid velocity, V , the density, ρ , the kinematic viscosity, ν , the magnetic permeability of vacuum, μ_0 , and the fluid electrical conductivity, σ . For most astrophysical objects, the global rotation rate, Ω , also plays an important role. Three independent dimensionless parameters thus govern the problem. We can

*Corresponding author. Email: petrelis@lps.ens.fr

choose the magnetic Reynolds number, R_m , the magnetic Prandtl number, P_m , and the Rossby number Ro :

$$R_m = \mu_0 \sigma V L, \quad P_m = \mu_0 \sigma \nu, \quad Ro = \frac{V}{L \Omega}. \quad (1)$$

For planets and stars as well as for all liquid metals in the laboratory, the magnetic Prandtl number is very small, $P_m < 10^{-5}$. Magnetic field self-generation can be obtained only for large enough values of R_m for which Joule dissipation can be overcome (for most known fluid dynamos, the dynamo threshold R_{mc} is roughly in the range 10–100). Therefore, the kinetic Reynolds number, $Re = VL/\nu = R_m/P_m$, is very large and the flow is strongly turbulent. This is of course the case of planets and stars which involve huge values of Re but is also true for dynamo experiments with liquid metals for which $Re > 10^5$. Direct numerical simulations are only possible for values of P_m orders of magnitude larger than the realistic ones for the sun, the Earth or laboratory experiments. First because it is not possible to handle a too large difference between the time scale of diffusion of the magnetic field and the one of momentum; second, a small P_m dynamo occurs for large Re and requires the resolution of the small spatial scales generated by turbulence. Strongly developed turbulence has also some cost for the experimentalist. Indeed, the power needed to drive a turbulent flow scales like $P \propto \rho L^2 V^3$ and we have

$$R_m \propto \mu_0 \sigma \left(\frac{PL}{\rho} \right)^{1/3}. \quad (2)$$

This formula has simple consequences: first, taking liquid sodium (the liquid metal with the highest electric conductivity), $\mu_0 \sigma \approx 10 \text{ m}^{-2} \text{ s}$, $\rho \approx 10^3 \text{ kg m}^{-3}$, and with a typical length scale $L \approx 1 \text{ m}$, we get $P \approx R_m^3$; thus a mechanical power larger than 100 kW is needed to reach a dynamo threshold of the order of 50. Second, it appears unlikely to ever operate experimental dynamos at R_m large compared with R_{mc} . Indeed, it costs 8 times more power to reach $2R_{mc}$ than to reach the dynamo threshold. In conclusion, most experimental dynamos should have the following characteristics:

- they bifurcate from a strongly turbulent flow regime,
- they operate in the vicinity of their bifurcation threshold.

Table 1. Relevant dimensionless parameters for some planets and the sun (from Zeldovich *et al.* 1983) and for laboratory fluid dynamos. (R_m has been evaluated on the full size even in the case of scale separation).

	P_m	R_m	Re	Ro^{-1}
Earth	5×10^{-7}	500	10^9	10^6
Jupiter	10^{-6}	10^6	10^{12}	10^6
Sun	5×10^{-8}	10^8	2×10^{15}	1
Experiments	10^{-5}	50	10^5 – 10^7	0–1

Although the values of R_m and P_m that can be obtained in laboratory experiments using liquid sodium are not too far from the ones of the Earth core, it would be very difficult to perform experiments with large R_m at Ro significantly smaller than unity whereas we have $Ro \approx 10^{-6}$ for the Earth core. The comparison is of course also difficult in the case of the sun: although Ro is of order one for the solar convection zone, R_m is more than six orders of magnitude larger than in any laboratory experiment. As said above, the situation is worse when direct numerical simulations are considered. We thus cannot claim that cosmic magnetic fields can be reproduced at the laboratory scale except if we can show that the dynamics of the magnetic field weakly depends on some dimensionless parameters.

As already mentioned, laboratory dynamos operate in the vicinity of the instability threshold but at very high values of the Reynolds number. This gives rise to a very interesting example of instability that differs in many respects from usual hydrodynamical instabilities. The dynamo bifurcation occurs from a base state which is fully turbulent. This may play a role on various aspects of the dynamo process and it raises several questions.

- What is the effect of turbulent velocity fluctuations on the dynamo onset? Will they favor or inhibit dynamo action? Can they change the nature of the bifurcation?
- Above onset, at which amplitude does the magnetic field saturate? Does it display an anomalous scaling with respect to the distance to threshold due to turbulent fluctuations?
- What are the statistical properties of the fluctuations of the magnetic field?

We will discuss this problem in connection with existing laboratory dynamo experiments. The first ones, performed in Karlsruhe and Riga, have been designed by taking into account the mean flow alone. Turbulent fluctuations have been inhibited as much as possible by a proper choice of boundary conditions. On the contrary, the VKS experiment has been first motivated by the study of the possible effects of turbulence on the dynamo instability.

The paper is organised as follows: in section 2, we recall the results of Karlsruhe and Riga experiments. Section 3 concerns the effect of small turbulent fluctuations on the dynamo threshold and emphasises the effect of the Reynolds number on the scaling law for the saturated magnetic field above threshold. Section 4 considers some questions related to dynamos generated by strongly turbulent flows, i.e. with less geometrical constraints than the Karlsruhe and Riga experiments. The results of the VKS experiment with counter-rotating impellers are presented in section 5. A possible dynamo mechanism for the VKS experiment together with some additional comments are presented in section 6. Finally, some open questions and other possible dynamo experiments are discussed in section 7.

2. The Karlsruhe and Riga experiments

The first homogeneous fluid dynamos have been operated in liquid sodium in Karlsruhe (Stieglitz and Müller 2001) using a flow in an array of pipes set-up in order to mimic a spatially periodic flow proposed by G.O. Roberts (1972), and in Riga (Gailitis *et al.* 2001) using a Ponomarenko-type flow (Ponomarenko 1973). We first recall the flow geometries and briefly review the results obtained by both groups.

2.1. The Karlsruhe experiment

The experiment in Karlsruhe, Germany, was motivated by a kinematic dynamo model developed by G.O. Roberts (Roberts 1972) who showed that various periodic flows can generate a magnetic field at large scale compared to the flow spatial periodicity. One of the cellular flows he considered is a periodic array of vortices with the same helicity. Flows with such topology drive an α -effect that can lead to dynamo action. This mechanism is quite efficient at self-generation (in the sense of generating a magnetic field at a low magnetic Reynolds number based on the wavelength of the flow).

A dynamo based on this mechanism was constructed and run with success in Karlsruhe. A sketch of the experiment is shown in figure 1(a). The flow is located in a cylindrical vessel of width 1.85 m and height $H = 0.7$ m. It contains 52 elementary cells placed on a square lattice. Each cell is made of two coaxial pipes: an helical baffle drives the helical flow in the outer cylindrical shell whereas the flow in the inner shell is axial. In two neighbouring cells, the velocities are opposite such that the helicity has the same sign in all the cells. Although the volume is finite instead of the infinite extension assumed by G. O. Roberts, the dynamo capability of the flow is not strongly affected in the limit of scale separation, i.e., when the size L of the full volume is large compared to the wavelength l of the flow (Busse *et al.* 1996). In this limit, the relevant magnetic Reynolds number involves the geometrical mean of the two scales as a length scale, and the geometrical mean of axial and azimuthal velocities as a velocity scale. However, it can be shown using simple arguments that it is not efficient to increase too much the scale separation if one wants to minimise the power needed to reach the dynamo threshold (Fauve and Pétrélis 2003). The flow is driven by three electromagnetic pumps and the axial and azimuthal velocities are independently controlled. The liquid sodium temperature is maintained fixed by three steam-evaporation heat exchangers. Measurements of the magnetic field were made

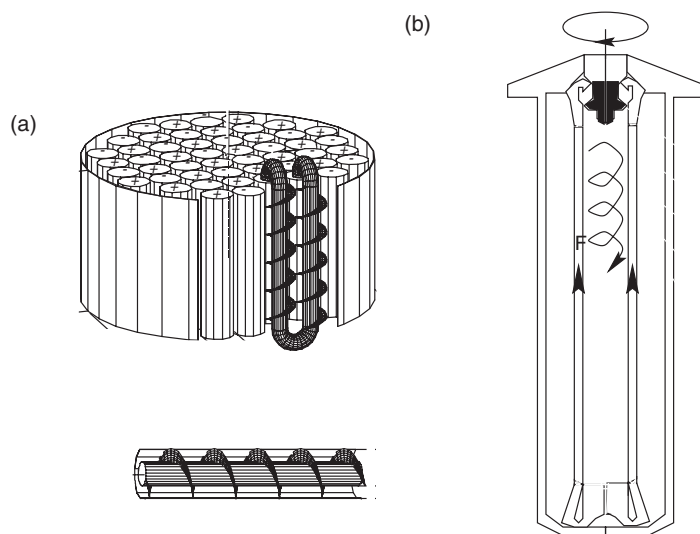


Figure 1. Schematics for the experiments from Karlsruhe (a) and Riga (b) which show how helical flow is forced by guiding the sodium through steel channels (from Stieglitz and Müller 2001 and Gailitis *et al.* 2001).

both locally with Hall-probes and globally using wire coils. Pressure drops in the pipe and local velocity measurements were also performed.

When the flow rates are large enough, a magnetic field is generated by dynamo action. The bifurcation is stationary and the magnetic field displays fluctuations caused by the small scale turbulent velocity field (see figure 2). This generation comes at a cost in the power necessary to drive the flow and the pressure drop increases.

Due to the Earth's magnetic field, the bifurcation is imperfect but both branches of the bifurcation can be reached by applying an external magnetic field, as displayed in figure 3. Among others, the experimentalists performed careful studies of the dependence of the dynamo threshold on the axial and helical flow rates and on the electrical conductivity that can be varied by changing the temperature. They also considered the effect of flow modulation on the dynamo threshold and studied the amplitude and the geometry of the magnetic field in the supercritical regime.

2.2. The Riga experiment

The experiment carried out by Gailitis *et al.* (2001) has been motivated by one of the simplest examples of a homogeneous dynamo found by Ponomarenko (1973). A conducting cylinder of radius R , embedded in an infinite static medium of the same conductivity with which it is in perfect electrical contact, is in solid body rotation at angular velocity Ω , and in translation along its axis at speed V . In an unbounded domain, this helical motion generates a travelling wave magnetic field. This Hopf bifurcation occurs for a minimum critical magnetic Reynolds number $R_{mc} = \mu_0 \sigma R \sqrt{(R\omega)^2 + V^2} = 17.7$ for an optimum Rossby number $Ro = V/(R\Omega) = 1.3$. We note that the maximum dynamo capability of the flow (R_{mc} minimum) is obtained

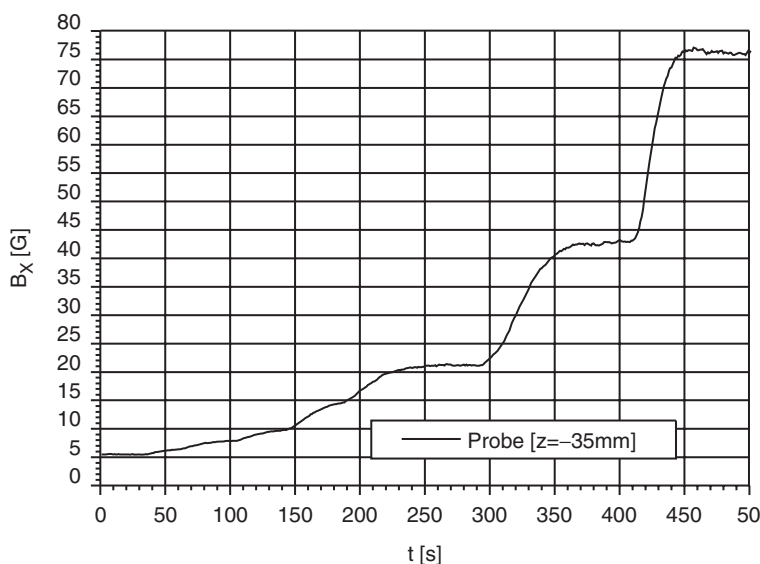


Figure 2. Time recording of one component of the magnetic field in the Karlsruhe experiment. The amplitude of the magnetic field increases after each increasing step of the flow rate of liquid sodium. Small fluctuations are visible once the magnetic field has saturated at a constant mean value. (Figure from Stieglitz and Müller 2002).

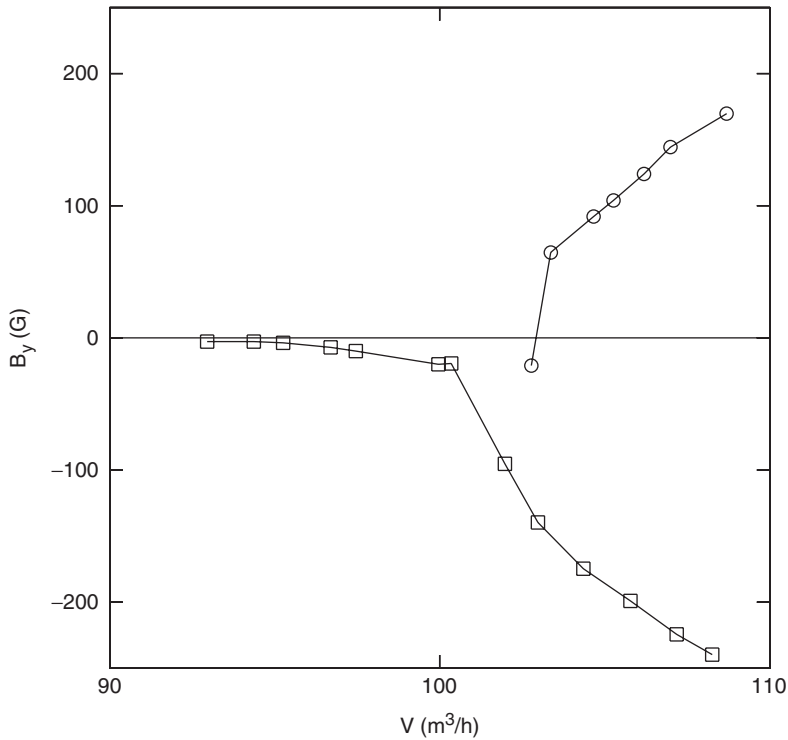


Figure 3. The magnetic field amplitude increases above the critical flow rate in the Karlsruhe experiment. Another branch of self-generation can be reached only by imposing an initial field. This other branch is disconnected from the main branch. The imperfection of the bifurcation has been ascribed to the Earth's field. (Figure from Stieglitz and M  ller 2002).

when the azimuthal and axial velocities are of the same order of magnitude ($Ro \sim 1$). This trend is often observed with more complex flows for which the maximum dynamo capability is obtained when the poloidal and toroidal flow components are comparable.

The experiment set up by the Riga group is sketched in figure 1(b). Their flow is driven by a single propeller, generating helical flow down a central cylindrical cavity. The return flow is in an annulus surrounding this central flow. The geometry of the apparatus as well as mean flow velocity profiles have been optimized in order to decrease the dynamo threshold. In particular, it has been found that adding an outer cylindrical region with liquid sodium at rest significantly decreases R_{mc} . This can be understood if the axial mean flow as well as the rotation rate of the azimuthal mean flow are nearly constant except in boundary layers close to the inner cylinder. Then, the induction equation being invariant under transformation to a rotating reference frame and under Galilean transformations, the presence of some electrical conductor at rest is essential as it is in the case of the Ponomarenko dynamo. The three cylindrical chambers are separated by thin stainless steel walls, which were wetted to allow currents to flow through them.

Figure 4 displays the growth and saturation of a time periodic magnetic field at high enough rotation rate. The nature of the bifurcation as well as dynamo growth rates have been found in good agreement with kinematic theory (Gailitis *et al.* 2002)

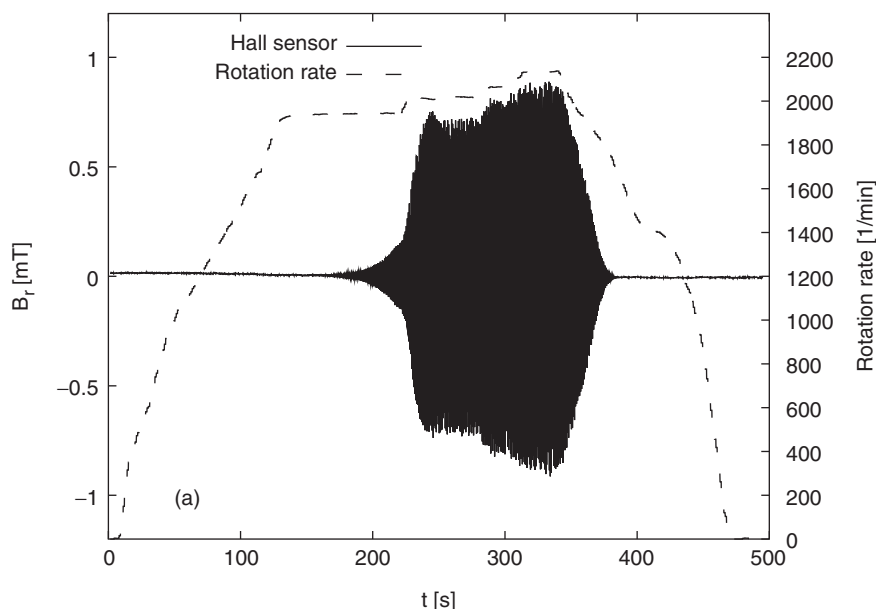


Figure 4. Time recording of the magnetic field from the Riga experiment. The dashed line gives the value of the rotation rate. The amplitude of roughly sinusoidal oscillations (not visible with the resolution of the picture) increases and then saturates when the rotation rate is increased above threshold (about 1850 rpm). The amplitude of saturation increases when the rotation rate is increased further. The dynamo switches off when the rotation rate is decreased below threshold (Figure from Gailitis *et al.* 2001).

that predicts a Hopf bifurcation of convective nature at onset. Note that this bifurcation can be affected by the ramping time scale of the propellor rotation rate (Knobloch 2007). In addition, the Riga group has made detailed observations of the magnetic field saturation value and the power dissipation needed to drive the flow. These measurements give indications of the effect of Lorentz forces in the flow in order to reach the saturated state. It has been found that one effect of the Lorentz force is to drive the liquid sodium in the outer cylinder in global rotation, thus decreasing the effective azimuthal velocity of the inner flow and therefore its dynamo capability. Dynamo generation does also correspond to an increase in the required mechanical power. However, a puzzling result is displayed in figure 5: the amplitude of the magnetic field for supercritical rotation rates does not seem to show the universal $\sqrt{R_m - R_{mc}}$ law. In addition, the form of the law seems to depend on the location of the measurement point. This is to some extent due to the absence of temperature control in the Riga experiment. Variations in temperature modify the fluid parameters (electrical conductivity, viscosity and density) and this should be taken into account by plotting the results in dimensionless form (Fauve and Lathrop 2005).

2.3. Lessons from the Karlsruhe and Riga experiments

Although there were no doubts about self-generation of magnetic fields by Roberts' or Ponomarenko-type laminar flows, these experiments have displayed several

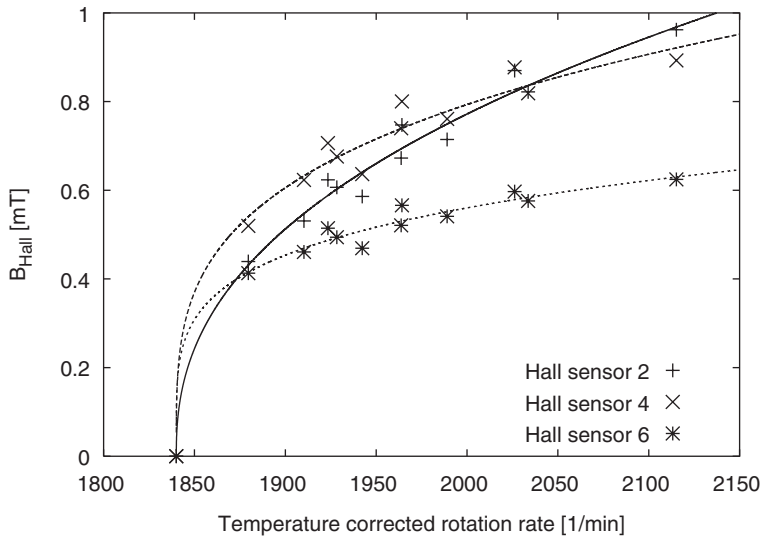


Figure 5. Magnetic field amplitude as the rotation rate is raised above the critical rotation rate. (Figure from Gailitis *et al.* 2003).

interesting features:

- the observed thresholds are in rather good agreement with theoretical predictions (Busse *et al.* 1996, Rädler *et al.* 1998, Gailitis *et al.* 2002) made by considering only the laminar mean flow and neglecting the small-scale turbulent fluctuations that are present in both experiments.
- The nature of the dynamo bifurcation, stationary for the Karlsruhe experiment or oscillatory (Hopf) in the Riga experiment, is also in agreement with laminar models.
- On the contrary, the saturation level of the magnetic field, due to the back reaction of the Lorentz force on the flow, cannot be predicted with a laminar flow model and different scaling laws exist in the supercritical dynamo regime depending on the magnitude of the Reynolds number (Pétrélis and Fauve 2001).
- Although secondary instabilities generating large scale dynamics of the magnetic field (such as field reversals for instance) have not been observed in the Karlsruhe and Riga experiments, small scale turbulent fluctuations of the magnetic field are well developed.

These observations raise the following questions:

- What is the effect of turbulence, or of the magnitude of the Reynolds number, on the dynamo threshold R_{mc} ? Is it possible to observe how R_{mc} depends on P_m for a dynamo generated by a strongly turbulent flow (by changing P_m in experiments with a given flow at different temperatures for instance)?
- What is the mechanism responsible for magnetic field fluctuations in the vicinity of the dynamo threshold: an on-off intermittency effect (Sweet *et al.* 2001) or chaotic advection of the mean magnetic field by the turbulent flow?
- What is the mechanism for field reversals? Is it possible to observe them in laboratory experiments?

3. Effect of turbulence on the dynamo threshold and saturation

3.1. Effect of small scale turbulent fluctuations on the dynamo threshold

As said above, dynamo experiments involve high Reynolds number flows and turbulent velocity fluctuations. Using the Reynolds decomposition, we write

$$\mathbf{V}(\mathbf{r}, t) = \overline{\mathbf{V}}(\mathbf{r}) + \tilde{\mathbf{v}}(\mathbf{r}, t), \quad (3)$$

where $\overline{\mathbf{V}}(\mathbf{r})$ is the mean flow and $\tilde{\mathbf{v}}(\mathbf{r}, t)$ are the turbulent fluctuations. The over-bar stands for a temporal average in experiments. The induction equation then becomes

$$\frac{\partial \mathbf{B}}{\partial t} = \nabla \times (\overline{\mathbf{V}} \times \mathbf{B}) + \nabla \times (\tilde{\mathbf{v}} \times \mathbf{B}) + \nu_m \nabla^2 \mathbf{B}, \quad (4)$$

where $\nu_m = 1/(\mu_0 \sigma)$ is the magnetic diffusivity. The Karlsruhe and Riga experiments have been designed by considering only the mean flow $\overline{\mathbf{V}}(\mathbf{r})$ in order to predict the value of the dynamo threshold. However, we observe that turbulent fluctuations $\tilde{\mathbf{v}}(\mathbf{r}, t)$ act as a random multiplicative forcing in the induction equation (4). It is well known, both from simple theoretical models (Stratonovich 1963, Graham and Schenzle 1985, Lücke and Schank 1985) and from experiments on different instability problems (Kabashima *et al.* 1979, Residori *et al.* 2001, Berthet *et al.* 2003, Pétrélis and Aumaître 2003, Pétrélis *et al.* 2005), that multiplicative noise generally shifts the bifurcation threshold. In addition, it sometimes modifies the dynamics of the unstable modes in the vicinity of threshold. In particular, multiplicative random forcing may generate intermittent bursting in the vicinity of instability onset (John *et al.* 1999, Berthet *et al.* 2003, Aumaître and Pétrélis 2003). This type of behaviour has been also observed with deterministic chaos instead of noise. It has been understood in the framework of blowout bifurcations in dynamical system theory (Platt *et al.* 1993), and has been observed in a numerical simulation of the MHD equations without external noise (Sweet *et al.* 2001). Note however that in these simulations, P_m is of order one, and the flow is chaotic at the dynamo threshold but not fully turbulent. We will use the same terminology “on-off intermittency” both for deterministic dynamical systems and systems with a noisy bifurcation parameter.

The effect of velocity fluctuations has been considered a long time ago in order to explain reversals of the magnetic field of the Earth as a result of statistical fluctuations of cyclonic convective cells (Parker 1969). Similar models using a noisy α -effect have been developed (Hoyng 1993). We will not study this type of problems here.

As said above, no significant shift in threshold with respect to computations taking into account only the mean flow have been observed in the Karlsruhe and Riga experiments. Bursting phenomena in the vicinity of threshold have not been reported either despite the existence of velocity fluctuations.

An explanation for the small shift in threshold has been given by Pétrélis (2002) and Fauve and Pétrélis (2003) as follows: in the limit of small fluctuations, one can calculate the threshold shift using a perturbation expansion. Let $\overline{\mathbf{V}}$ be the average velocity field at onset, and \mathbf{B} the neutral mode of the instability. Let $\mathbf{V}^{(0)}$ be the flow leading to the neutral mode $\mathbf{B}^{(0)}$ when there is no velocity fluctuations. Our aim is to find how the dynamo threshold of the velocity field $\mathbf{V}^{(0)}$ is modified in the presence of small turbulent fluctuations. We write $\tilde{\mathbf{v}} = \delta \mathbf{v}$ where δ is a small parameter that measures

the intensity of the turbulent fluctuations so that the amplitude of \mathbf{v} is of order one. The neutral mode is likely to be slightly modified by the fluctuations as well as the dynamo threshold. We expand \mathbf{B} and $\bar{\mathbf{V}}$ in powers of δ :

$$\mathbf{B} = \mathbf{B}^{(0)} + \delta \mathbf{B}^{(1)} + \delta^2 \mathbf{B}^{(2)} + \dots, \quad \bar{\mathbf{V}} = \mathbf{V}^{(0)}(1 + c_1 \delta + c_2 \delta^2 + \dots),$$

$\mathbf{B}^{(i)}$ are the corrections at order i to the neutral mode due to the presence of the turbulent fluctuations. c_i are constants that express the shift in the dynamo threshold caused by turbulence. We emphasise that we study the modification of the dynamo threshold of a mean flow with prescribed geometry due to the presence of fluctuations. When one inputs these expressions in equation (4), the zeroth order part can be written

$$L\mathbf{B}^{(0)} \equiv \frac{\partial \mathbf{B}^{(0)}}{\partial t} - \nabla \times (\mathbf{V}^{(0)} \times \mathbf{B}^{(0)}) - \nu_m \nabla^2 \mathbf{B}^{(0)} = \mathbf{0}. \quad (5)$$

This is the laminar dynamo problem. By hypothesis, the instability onset is the one without turbulent perturbation. At next order in δ we get

$$L\mathbf{B}^{(1)} = c_1 \nabla \times (\mathbf{V}^{(0)} \times \mathbf{B}^{(0)}) + \nabla \times (\mathbf{v} \times \mathbf{B}^{(0)}). \quad (6)$$

We now introduce a scalar product $\langle f|g \rangle$ and calculate L^+ the adjoint of L . As $L\mathbf{B}^{(0)} = 0$, L^+ also has a nonempty kernel. Let \mathbf{C} be in this kernel. Then

$$\langle \mathbf{C}|L\mathbf{B}^{(1)} \rangle = \langle L^+\mathbf{C}|\mathbf{B}^{(1)} \rangle = 0 \quad (7)$$

and this solvability condition gives the first order correction in the threshold

$$c_1 = - \frac{\langle \mathbf{C}|\nabla \times (\mathbf{v} \times \mathbf{B}^{(0)}) \rangle}{\langle \mathbf{C}|\nabla \times (\mathbf{V}^{(0)} \times \mathbf{B}^{(0)}) \rangle}. \quad (8)$$

We use a scalar product in which the average over the realisations of the perturbation is made. In that case, the average over the realisations of $\langle \mathbf{C}|\nabla \times (\mathbf{v} \times \mathbf{B}^{(0)}) \rangle$ is proportional to the average of \mathbf{v} , the value of which is zero by hypothesis. Thus, the dynamo threshold is unchanged up to first order in δ , $c_1 = 0$. This result is obvious in many simple cases. For instance if $\tilde{\mathbf{v}}$ is sinusoidal in time, the threshold shift cannot depend on the phase which implies that it is invariant if $\tilde{\mathbf{v}} \rightarrow -\tilde{\mathbf{v}}$. This is also true if $\tilde{\mathbf{v}}$ is a random noise with equal probabilities for the realisations $\tilde{\mathbf{v}}$ and $-\tilde{\mathbf{v}}$. Note however that simple symmetry arguments do not apply for asymmetric fluctuations about the origin although the threshold shift vanishes to leading order if the fluctuations have zero mean.

To calculate the next order correction, we write equation (4) at order two in δ and get

$$L\mathbf{B}^{(2)} = c_2 \nabla \times (\mathbf{V}^{(0)} \times \mathbf{B}^{(0)}) + \nabla \times (\mathbf{v} \times \mathbf{B}^{(1)}). \quad (9)$$

We then get the second order correction

$$c_2 = -\frac{\langle \mathbf{C} | \nabla \times (\mathbf{v} \times \mathbf{B}^{(1)}) \rangle}{\langle \mathbf{C} | \nabla \times (\mathbf{V}^{(0)} \times \mathbf{B}^{(0)}) \rangle}, \quad (10)$$

where $\mathbf{B}^{(1)}$ is solution of

$$L\mathbf{B}^{(1)} = \nabla \times (\mathbf{v} \times \mathbf{B}^{(0)}). \quad (11)$$

Here, there is no simple reason for the correction to be zero. Its computation requires the resolution of equation (11). In some simple cases, an analytical expression for c_2 can be calculated and both signs can be found, thus showing that fluctuations can in general increase or decrease the dynamo threshold (Pétreliis and Fauve 2006).

We have thus obtained that when the amplitude δ of turbulent fluctuations is small, the modification of the dynamo threshold is at least quadratic in δ . Consequently, we can understand why the thresholds measured in the Karlsruhe and Riga experiments are very close to the predictions using the mean flow $\bar{\mathbf{V}}$ and thus ignoring turbulent fluctuations (the order of magnitude of the level of turbulent fluctuations related to the mean flow is certainly less than 10% in these experiments). The problem is more complex for experiments with unconstrained flows for which large scale fluctuations can be of the same order as the mean flow. We will consider it in the section about “turbulent dynamos”.

3.2. Scaling laws for magnetic energy density in the vicinity of threshold

In order to describe the saturation of the magnetic field above the dynamo threshold, we need to take into account its back reaction on the velocity field. We thus have to solve the induction and Navier–Stokes equations, which we restrict to incompressible flows ($\nabla \cdot \mathbf{V} = 0$),

$$\frac{\partial \mathbf{B}}{\partial t} = \nabla \times (\mathbf{V} \times \mathbf{B}) + \frac{1}{\mu_0 \sigma} \nabla^2 \mathbf{B}, \quad (12)$$

$$\frac{\partial \mathbf{V}}{\partial t} + (\mathbf{V} \cdot \nabla) \mathbf{V} = -\nabla \left(\frac{p}{\rho} + \frac{\mathbf{B}^2}{2\mu_0} \right) + \nu \nabla^2 \mathbf{V} + \frac{1}{\mu_0 \rho} (\mathbf{B} \cdot \nabla) \mathbf{B}. \quad (13)$$

The flow is created, either by moving solid boundaries or by a body force added to the Navier–Stokes equation. We do not consider global rotation ($\Omega = 0$). We have to develop equations (12, 13) close to the dynamo threshold in order to derive an amplitude equation for the growing magnetic field. If the dynamo bifurcation is found supercritical, this allows the calculation of the saturated mean magnetic energy density $\langle B^2 \rangle / 2\mu_0$, where $\langle \cdot \rangle$ stands for average in both space and time in this section.

Thus, even in the simplest configuration, the problem involves three dimensionless parameters. One can choose, the magnetic Reynolds number, R_m , the magnetic

Prandtl number, P_m , and the ratio of the mean magnetic to kinetic energy density, leading to the following form of law

$$\frac{\langle B^2 \rangle}{\mu_0} = \rho \langle V^2 \rangle f(R_m, P_m). \quad (14)$$

In general, the analytic determination of f using weakly nonlinear perturbation theory in the vicinity of the dynamo threshold is tractable only in the unrealistic case $P_m \gg 1$ such that the dynamo bifurcates from a laminar flow ($Re \ll 1$). For $P_m \ll 1$, a lot of hydrodynamic bifurcations occur first and the flow becomes turbulent before the dynamo threshold that occurs for $Re \gg 1$. We will briefly recall the scaling laws that are expected in both limits (for more details, see P  tr  lis and Fauve 2001).

3.2.1. Saturation in the low Re limit. At small Re , the Lorentz force should be balanced by the viscous force as it is larger than the inertial one in (13). When the magnetic field bifurcates above a critical velocity amplitude V_c , it thus generates a velocity modification of order δV given by

$$\nu \frac{\delta V}{L^2} \propto \frac{B^2}{\rho \mu_0 L}. \quad (15)$$

If this bifurcation is supercritical, we expect saturation for δV of the order of the distance to criticality $V - V_c$. In the bifurcation analysis, this balance results from the solvability condition. We thus obtain

$$\langle B^2 \rangle \propto \frac{\rho \nu}{\sigma L^2} (R_m - R_{mc}). \quad (16)$$

Analytic calculations in the small Re limit have been performed both for the Roberts flow (Gilbert and Sulem 1990, Busse and Tilgner 2001) and Ponomarenko type flows (Nu  ez *et al.* 2001). In the case of the Roberts flow for which there are two spatial scales, the flow periodicity l and the size L of the full flow volume, the equation for $\langle B^2 \rangle$ in the limit $L \gg l$ takes the form

$$\langle B^2 \rangle \propto \frac{\rho \nu}{\sigma l^2} (R_m - R_{mc}), \quad (17)$$

with $R_m = \mu_0 \sigma \sqrt{UVLl}$ where U and V are respectively the axial and azimuthal typical velocities. The occurrence of l instead of L results from the balance between the Stokes and the Lorentz forces that both imply the small scale. The largest contribution to the current density is indeed the one associated to the small scale magnetic field in the limit of scale separation.

More surprisingly, the basic property of this ‘‘laminar scaling’’, i.e., B^2 proportional to ν , or $B^2/\mu_0 \rho V^2 \propto 1/Re$ in dimensionless form, subsists in the case of some rotating flows (Childress and Soward 1972, Soward 1974). Equation (16) is known as the ‘‘weak field scaling’’ of the Earth dynamo (Roberts 1988). The same property has been also found for a smooth helical flow in the limit $Re \gg R_m \gg 1$ (Bassom and Gilbert 1997).

3.2.2. Saturation in the large Re limit. At large Re , balancing the Lorentz force with the inertial one gives

$$\frac{V_c \delta V}{L} \propto \frac{B^2}{\rho \mu_0 L}. \quad (18)$$

Then, using $\delta V \propto V - V_c$, we obtain the large Re scaling

$$\langle B^2 \rangle \propto \frac{\rho}{\mu_0 (\sigma L)^2} R_{mc} (R_m - R_{mc}). \quad (19)$$

The dimensionless group $\langle B^2 \rangle \mu_0 (\sigma L)^2 / \rho$ is known as the Lundquist number.

The form of (19) can be easily found by dimensional arguments. For $P_m \ll 1$, the Ohmic dissipative scale, $l_\sigma = L R_m^{-3/4}$, is much larger than the Kolmogorov scale, $l_K = L Re^{-3/4}$. Thus, the magnetic field grows at scales much larger than l_K and does not depend on kinematic viscosity. Then, we can discard the dependence of f on P_m in (14). In the vicinity of dynamo threshold, V is not a free parameter but is such that $\mu_0 \sigma V L \approx R_{mc}$. We obtain

$$\langle B^2 \rangle \propto \frac{\rho}{\mu_0 (\sigma L)^2} f(R_m). \quad (20)$$

The scalings for large and small Re differ by a factor $R_{mc}/P_m \approx 10^6$ for experiments using liquid sodium ($P_m \approx 10^{-5}$). It may be instructive to replace ν by the turbulent viscosity, $\nu_T \propto VL$ (respectively $\nu_T \propto V l$ in the case of scale separation) in the laminar scaling (16). Using $V \approx R_{mc}/\mu_0 \sigma L$, we have

$$\langle B^2 \rangle \propto \frac{\rho \nu_T}{\sigma L^2} (R_m - R_{mc}) \propto \frac{\rho}{\mu_0 (\sigma L)^2} (R_m - R_{mc}). \quad (21)$$

We thus recover the turbulent scaling. However, the above analysis does not require any assumption about the expression of the turbulent viscosity and is thus clearer.

3.2.3. Magnetic energy density of the Karlsruhe and Riga dynamos. The Lundquist number, $\langle B^2 \rangle \mu_0 (\sigma r)^2 / \rho$ where r is the radius of each cylinder of the Karlsruhe experiment, is plotted as a function of R_m in figure 6 for two different ratios of the axial to azimuthal flows. The large scale magnetic field being the dominant component and slowly varying in space, its local value thus gives a reasonable estimate of the mean energy density. The choice of the small scale r instead of the full size of the flow in the Lundquist number results from equation (17). R_m has been defined using the geometrical mean of the axial and helical velocities as velocity scale but the height of the cylindrical volume $H = 0.7$ m has been taken as length scale. The later choice is somewhat arbitrary but allows a simple comparison with the other fluid dynamos.

Figure 6 shows that the dynamo threshold depends on the axial to azimuthal flow ratio although its leading order effect has been taken into account in the definition of the velocity scale in R_m . This may result from the expulsion of the transverse

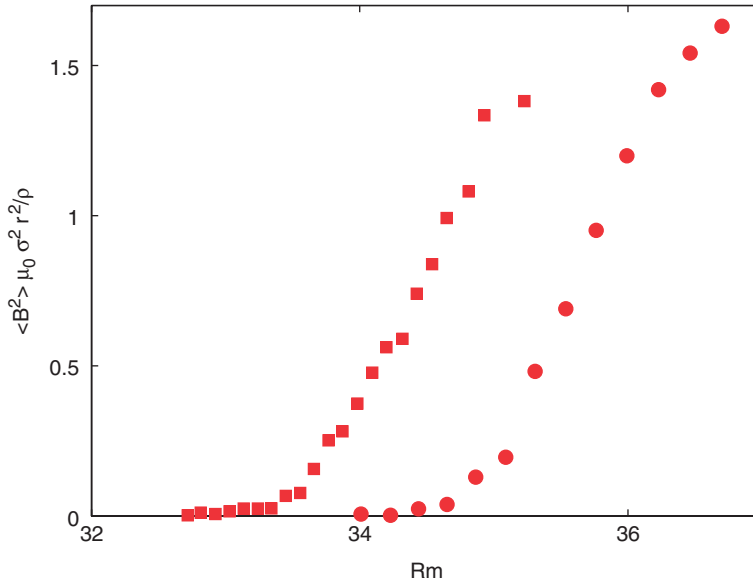


Figure 6. Dimensionless magnetic energy density $\langle B^2 \rangle \mu_0 \sigma^2 r^2 / \rho$ as a function of the magnetic Reynolds number R_m for the Karlsruhe experiment. The different symbols are associated to different ratios of azimuthal to axial velocity. R_m is varied through change in the temperature leading to a variation of the electrical conductivity (data from Müller *et al.* 2004).

magnetic field by the azimuthal flow. Another possible explanation comes from the geometry of the helical flow. Indeed, part of the helical flow contributes to the axial flow. Taking this component into account in the definition of R_m could decrease the difference between critical magnetic Reynolds numbers. On the contrary, the slope of the bifurcation curve does not seem to be strongly affected by the axial to azimuthal flow ratio.

Figure 7 displays the dynamo bifurcation using the same parameters for the Riga experiment. The Lundquist number as well as R_m are defined using the radius $R = 0.125\text{m}$ of the inner cylinder. The two curves are related to probes at different locations. We observe that the imperfection ascribed to the Earth's magnetic field in the Karlsruhe experiment does not exist in the Riga experiment. A constant external field is not resonant with the neutral mode that is a travelling wave and thus does not lead to any imperfection. Other measurements (not shown here) made at different spatial locations (see figure 5) have displayed smaller values of the magnetic field that is concentrated in the vicinity of the shear for a Ponomarenko-type dynamo. Multiple point measurements and averaging thus should be made in order to have a better evaluation of the mean magnetic energy density in the flow volume. Fortunately, the difference between the predictions (16) and (19) is so large that rough order of magnitude estimates of $\langle B^2 \rangle$ are enough. Taking into account the qualitative nature of our analysis in section 3.2, we conclude that the large Re scaling is in agreement with the experimental observations whereas the “laminar scaling” predicts a field that is orders of magnitude too small. We thus note that Karlsruhe and Riga experiments display an interesting feature: turbulent fluctuations can be neglected when computing the dynamo threshold whereas the high value of Re has a very

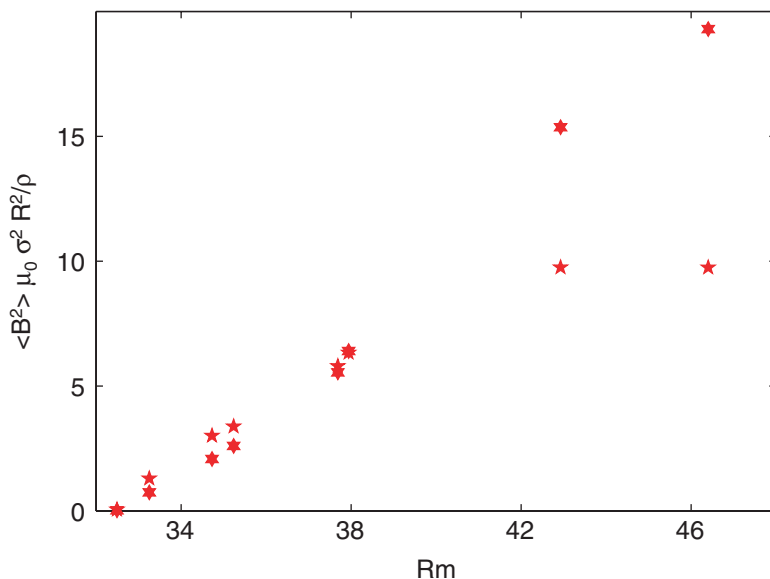


Figure 7. Dimensionless magnetic energy density $\langle B^2 \rangle \mu_0 \sigma^2 R^2 / \rho$ as a function of the magnetic Reynolds number R_m for the Riga experiment. The different values for same R_m are associated to different probe positions (data courtesy of Franck Stefani).

strong effect on the amplitude of the saturated magnetic energy density above the dynamo threshold.

4. Laminar versus turbulent dynamos

In a fully developed turbulent flow in a compact domain, i.e., without any mean flow prescribed by strong geometrical constraints, large scale fluctuations are generally of similar order of magnitude as the mean flow. Then, we cannot a priori expect that the dynamo computed as if it were generated by $\bar{\mathbf{V}}(\mathbf{r})$ alone can describe the observations as in the limit of small fluctuations considered in section 3.1. We thus propose the following definition: we call “laminar” a fluid dynamo which generates a magnetic field that displays the same characteristics as the one computed as if the mean flow $\bar{\mathbf{V}}(\mathbf{r})$ were acting alone. We mean by characteristics, the geometry of the mean field lines, the nature of the bifurcation (stationary, Hopf, etc.) and the related dynamics of the large scale field, the approximate value of R_{mc} , etc. Otherwise, the dynamo is called turbulent, which means that turbulent velocity fluctuations $\tilde{\mathbf{v}}(\mathbf{r}, \mathbf{t})$ qualitatively modify the nature of the bifurcation obtained with $\bar{\mathbf{V}}(\mathbf{r})$ alone. This of course does not mean that $\bar{\mathbf{V}}(\mathbf{r})$ has no effect on the dynamo process. This would remain true even if $\bar{\mathbf{V}}(\mathbf{r})$ alone has no dynamo capability.

4.1. Turbulent fluctuations and the shift of the dynamo threshold

It has been believed that studying the dynamo generated by the mean flow can often provide a leading order description of a fluid dynamo even in the presence of

large fluctuations. As just said, this is far from being obvious, but in that case, a natural question is related to the effect of turbulent fluctuations on threshold as considered in section 3.1 in the limit of small fluctuations. There exists no general answer to this question. Even in the limit of scale separation, it is known that the role of turbulent fluctuations may be twofold: on one hand, they decrease the effective electrical conductivity and thus inhibit the dynamo action generated by $\bar{\mathbf{V}}(\mathbf{r})$ by increasing Joule dissipation; on the other hand, they may generate a large scale magnetic field through the “ α -effect” (Moffatt 1978, Krause and Rädler 1980) or higher order similar effects even if $\bar{\mathbf{V}}(\mathbf{r}) = \mathbf{0}$. However, most natural flows do not involve any clear-cut scale separation, and it has been recently shown in several numerical simulations that the “ α -effect” may be very weak even for flow configurations involving large helicity where it could be expected to drive an efficient large scale magnetic field (Cattaneo and Hughes 2006, Hughes and Cattaneo 2007).

The effect of turbulent fluctuations on the dynamo threshold has been also studied with direct numerical simulation of the Taylor–Green flow, but with different outcomes: the observed threshold has been found to increase in the presence of large scale fluctuations (Laval *et al.* 2006) whereas it has been observed to correspond to some threshold corresponding to the mean flow alone (Ponty *et al.* 2005, 2007). It should be emphasised that these direct simulations, as well as the previous ones about the “ α -effect”, are not performed with small enough values of P_m so that one must be careful when using them to understand laboratory experiments.

In order to try to clarify this issue, it is instructive to consider the evolution equation of the magnetic energy

$$\frac{d}{dt} \int \frac{B^2}{2\mu_0} = \int (\mathbf{V} \times \mathbf{B}) \cdot \mathbf{j} d^3x - \int \frac{j^2}{\sigma} d^3x, \quad (22)$$

where \mathbf{j} is the current density ($\mu_0 \mathbf{j} \approx \nabla \times \mathbf{B}$ in the MHD approximation). At the dynamo threshold, the first term on the right hand side, the amplification term, should be equal to the second one that corresponds to Ohmic dissipation. If we assume that this is achieved in the absence of fluctuations, we observe that turbulent fluctuations can increase the dynamo threshold through two different types of mechanism: the most obvious one results from an increase of Ohmic losses due to the generation of magnetic field at small scales by advection of field lines by turbulent eddies. The second one is a loss of the efficiency of field amplification. The amplification term depends on the relative orientation of \mathbf{V} , \mathbf{B} and \mathbf{j} , thus fluctuations in direction of these vectors can decrease it. We briefly discuss these two phenomena.

The increase of Ohmic dissipation due to turbulence primarily depends on the value of the magnetic Reynolds number related to the corresponding velocity fluctuations, $\mu_0 \sigma l v_{rms}$ where v_{rms} the rms value of velocity fluctuations $\tilde{\mathbf{v}}$ and l is their integral scale. If $\mu_0 \sigma l v_{rms} \approx 1$ or smaller, the fluctuations of the magnetic field due to turbulence have a spectrum of the form $|\hat{B}|^2 \propto (\mu_0 \sigma B_0)^2 k^{-2} |\hat{v}|^2 \propto (\mu_0 \sigma B_0)^2 \epsilon^{2/3} k^{-11/3}$ where \mathbf{B}_0 is the large scale magnetic field and $\epsilon = V^3/L$ is the energy flux per unit mass (Golitsyn 1960, Moffatt 1961). This spectrum being steeper than k^{-3} , currents related to the large scale magnetic field are dominant and Ohmic dissipation is hardly increased by turbulence. The dynamo threshold is only slightly shifted as explained in section 3

and observed in Karlsruhe and Riga experiments for which $\mu_0 \sigma l v_{rms}$ is of order one or less.

The situation strongly differs in flows without geometrical constraints for which Kolmogorov-type turbulent fluctuations exist up to the size L of the fluid container and have a rms value of the same order as the mean flow. The magnetic Reynolds number of turbulent fluctuations is thus of the same order as the one related to the mean flow, R_m , and $R_m > 10$ at threshold. Then there exists an inertial magnetic range, $l_\sigma = LR_m^{-3/4} < l < L$, in which $|\hat{B}|^2$ follows a different scaling law. Unfortunately, no theoretical prediction for $|\hat{B}|^2$ is available in the vicinity of the dynamo threshold. Note that predictions for spectra of magnetohydrodynamic turbulence such as, $|\hat{B}|^2 \propto (\rho\mu_0)^{3/4}(\epsilon B_0)^{1/2}k^{-3/2}$ (Iroshnikov 1964, Kraichnan 1965) followed by many other models based on Alfvén wave turbulence (for a review, see Verma 2004), require an applied field value B_0 larger than the one achieved in the vicinity of the dynamo threshold. Similarly, the Kolmogorov-type spectrum $|\hat{B}|^2 \propto \rho\mu_0\epsilon^{2/3}k^{-5/3}$, recently proposed for small P_m turbulent dynamos at large R_m (Fauve and Pétrelis 2007), is not expected close to threshold.

Dimensional analysis lead to

$$|\hat{B}|^2 \propto \rho\mu_0 \langle V^2 \rangle k^{-1} f(R_m, kl_\sigma), \quad (23)$$

where f is an arbitrary function. In the vicinity of the dynamo threshold it is expected to become

$$|\hat{B}|^2 \propto \rho\mu_0 \langle V^2 \rangle k^{-1} (R_m - R_{mc}) g(kl_\sigma), \quad (24)$$

where g is another arbitrary function. Let us assume the following form of the spectrum of the magnetic fluctuations:

$$\begin{aligned} |\hat{B}|^2 &= A(k/k_\sigma)^\alpha & \text{if } k/k_\sigma < 1 \\ &= A(k/k_\sigma)^{-11/3} & \text{if } k/k_\sigma > 1, \end{aligned} \quad (25)$$

where α is an exponent that depends on the regime under consideration, $k_\sigma = 2\pi/l_\sigma$, and A is obtained by $\int |\hat{B}|^2 dk = \langle B^2 \rangle$. For $\alpha > -1$, one gets $A \propto \langle B^2 \rangle LR_m^{-3/4}$ and for $\alpha < -1$, $A \propto \langle B^2 \rangle LR_m^{3\alpha/4}$.

Then using

$$\frac{1}{\sigma} \langle j^2 \rangle = \frac{1}{\sigma} \int |\hat{j}|^2 dk \propto \frac{1}{\mu_0^2 \sigma} \int k^2 |\hat{B}|^2 dk, \quad (26)$$

we estimate Ohmic dissipation

$$\begin{aligned} \frac{1}{\sigma} \langle j^2 \rangle &\propto \frac{\langle B^2 \rangle}{\mu_0^2 \sigma L^2} Rm^{3/2} & \text{if } \alpha > -1, \\ &\propto \frac{\langle B^2 \rangle}{\mu_0^2 \sigma L^2} \frac{Rm^{3/2}}{\log(Rm)} & \text{if } \alpha = -1, \end{aligned}$$

$$\begin{aligned} &\propto \frac{\langle B^2 \rangle}{\mu_0^2 \sigma L^2} Rm^{(9+3\alpha)/4} && \text{if } -3 < \alpha < -1, \\ &\propto \frac{\langle B^2 \rangle}{\mu_0^2 \sigma L^2} && \text{if } \alpha < -3. \end{aligned} \quad (27)$$

The next step is to relate $\langle B^2 \rangle$ to $\langle B \rangle$. Following Moffatt (1961), one can assume that $\langle B \rangle$ imposes the value of the spectrum at k_L so that $\langle B \rangle^2 \approx A(k_L/k_\sigma)^\alpha k_L$. Then $\langle B^2 \rangle \propto \langle B \rangle^2 Rm^{(9+3\alpha)/4}$ if $\alpha > -1$ and $\langle B^2 \rangle \propto \langle B \rangle^2$ otherwise. One gets

$$\begin{aligned} \frac{1}{\sigma} \langle j^2 \rangle &\propto \frac{\langle B \rangle^2}{\mu_0^2 \sigma L^2} Rm^{(9+3\alpha)/4} && \text{if } \alpha > -3, \\ &\propto \frac{\langle B \rangle^2}{\mu_0^2 \sigma L^2} && \text{if } \alpha < -3, \end{aligned} \quad (28)$$

where $\langle B \rangle^2/(\mu_0^2 \sigma L^2)$ is the dissipation in the laminar regime. We thus obtain that the effect of turbulent fluctuations is to increase Ohmic dissipation by a factor $R_m^{5/2}$ if $\alpha = 1/3$ according to Moffatt (1961) or by a factor $R_m^{3/2}$ if $\alpha = -1$ according to Ruzmaikin and Shukurov (1982). To sum up, any spectrum less steep than k^{-3} in the interval $[k_L, k_\sigma]$ leads to an enhancement of Ohmic dissipation.

Fluctuations can also increase the dynamo threshold in the absence of any turbulent cascade. A simple example has been provided by Pétrélis and Fauve (2006) by considering phase fluctuations of the G.O. Roberts flow

$$\mathbf{V} = \begin{pmatrix} V(\cos(ky + \phi) - \cos(kz + \psi)) \\ U \sin(kz + \psi) \\ U \sin(ky + \phi) \end{pmatrix}, \quad (29)$$

where ψ and ϕ are two functions that depend on time only, or

$$\mathbf{V} = \begin{pmatrix} V(\cos(ky + \phi) - \cos(kz + \psi)) \\ U \sin(kz + \psi) - (V/k) \partial_x \phi \cos(ky + \phi) \\ U \sin(ky + \phi) + (V/k) \partial_x \psi \cos(kz + \psi) \end{pmatrix}, \quad (30)$$

where ϕ and ψ depend on x only. Both flows involve phase fluctuations, i.e., motions of the eddies. In the first case, this amounts to switch the origin of the flow in time. In the second case, spatial fluctuations of the eddies along the x -axis are considered, the additional terms in the second and third components of the velocity field are just ensuring the incompressibility of the flow. In the limit of scale separation, and assuming that the phase gradients in time (respectively in space) are small enough, it has been shown that these large scale fluctuations always increase the dynamo threshold of the G.O. Roberts flow. The above examples are simple enough to compute how fluctuations increase the threshold of the neutral mode generated by the mean flow alone. They also show that even if this threshold is increased, different modes that cannot be amplified by the mean flow, can be generated by the time

dependent flow. It has been indeed shown that when ψ and ϕ are sinusoidal functions of time in the first flow given above, fast dynamo modes are generated (Galloway and Proctor 1992).

In conclusion, no general statement about the effect of fluctuations on the dynamo threshold can be made. When fluctuations occur at small scale and are of small amplitude such that their magnetic Reynolds number is small, their effect on the neutral mode generated by the mean flow alone is small and can be computed perturbatively. The shift in threshold occurs at second (or higher) order. On the contrary, for Kolmogorov type turbulence with large scale fluctuations of the same order as the mean flow, it is expected that Ohmic dissipation is increased and the efficiency of the amplification mechanism of the neutral mode generated by the mean flow alone can be decreased. However, other modes may be selectively amplified due to the presence of fluctuations. These observations question the validity of dynamo models based only on the mean flow, thus neglecting the effect of large scale turbulent fluctuations. Experimental studies of the transport of a localized magnetic field by a turbulent flow have also shed light on the effect of fluctuations (Volk *et al.* 2006b). In particular, they show a loss of the magnetic field orientation in the transport process that may lower the efficiency of the field amplification as stated before.

4.2. On-off intermittency

In addition to a shift of threshold, the nature of the bifurcation can be modified in the presence of fluctuations. The simplest example is provided by the phenomenon of on-off intermittency. On-off intermittent behaviour is a common feature for bifurcating systems subjected to multiplicative noise. Consider a system close to an instability threshold. Multiplicative noise induces fluctuations of the instantaneous departure from onset. If the fluctuations are large compared to the mean departure from onset, the average over a time interval T of the instantaneous departure from onset can be negative even for long duration T . Then the amplitude of the unstable mode tends to zero (off-phase) before the average departure from onset turns back to a positive value and the unstable mode reaches amplitudes where nonlinearities saturate its growth (on-phase). This is a simple mechanism that leads to the random succession of phases where the unstable system is either close to its formerly stable solution or reaches values controlled by non-linearities.

Up to now this behaviour has not been displayed by experimental dynamos. Two key elements have been identified that can limit the ability for a dynamo to exhibit an on-off intermittent magnetic field.

The fluctuations that drive the off-phases are long time fluctuations. For simple dynamical systems, it has been shown that the on-off intermittent behaviour is controlled by the zero frequency component of the spectrum of the multiplicative noise (Aumaitre *et al.* 2005, Aumaitre *et al.* 2006). Indeed, on-off intermittency takes place when the ratio between the departure from onset and the zero frequency component of the noise is small. It seems reasonable to assume that for dynamos, fluctuations of the velocity field at very small frequencies are required. It is probable that the currently working dynamos do not have enough low frequency fluctuations to generate an on-off intermittent magnetic field.

Another effect that can play a role is the imperfectness of the bifurcation. It is important for the mechanism of on-off intermittency that when the system evolves

towards the off-phase, the effect of the noise term vanishes. If the bifurcation is imperfect, the deterministic solution does not tend to a zero magnetic field solution but to the imperfect branch. Then the effect of multiplicative noise does not vanish. This generates fluctuations that can destroy the intermittent regime (P  tr  lis and Auma  tre 2006). Note that the effect is the same as for additive noise that also leads to a disappearance of on–off intermittency (Platt *et al.* 1994). In the dynamo context, even though the fluctuations remain multiplicative, the imperfectness of the bifurcation can be the source of the fluctuations that prevent the observation of on–off intermittency.

A source of imperfectness for experimental dynamos is the ambient magnetic field of the Earth and of the possibly magnetised parts of the experiment, as for instance the propellers in the VKS experiment. It might be helpful to screen these ambient fields in order to observe on–off intermittent dynamos.

To sum up, in order to favour on–off intermittency above the dynamo onset, it is important to lower the source of imperfectness of the bifurcation, for instance by screening the ambient fields and it is important to have a velocity field that displays large fluctuations at low frequencies. Then, slightly above the dynamo onset, on–off intermittency could be possibly observed.

4.3. Sodium experiments with weakly constrained flows

Early experiments have been performed by Lehnert (1957). A swirling flow has been generated by rotating a disk in a cylindrical vessel containing 58 l of liquid sodium. Although a self-generated dynamo regime has not been reached, induction measurements have been performed with an applied axial field. The generation of a toroidal (ω -effect) and poloidal field components have been observed. Another early sodium experiment has been motivated by planetary dynamos for which tidal forces have been considered as a possible source of power driving the dynamo (Malkus 1968). Precession of a rotating cylinder filled with liquid sodium has been studied by Gans (1970). The rotation rate was increased up to 3600 rpm for a precession rate of 50 rpm. An external magnetic field amplification has been reported but no self-generation.

Flows in spherical geometry are currently investigated in two dynamo experiments in the USA. The Wisconsin experiment (Forest *et al.* 2002, Nornberg *et al.* 2006, Spence *et al.* 2006) is operational: the spherical shell is motionless and the fluid is driven by two propellers. This set-up is to be linked with numerical work by Dudley and James (1989). No dynamo action has been observed so far in the Wisconsin flow. Experiments in a similar geometry but at a smaller scale have been performed in Maryland (Peffley *et al.* 2000).

Other sodium experiments, motivated by the context of the geodynamo, involve system-wide rotation. There is a widespread belief that global rotation may assist generation by lowering the critical Reynolds number. A spherical Couette flow has been studied in Grenoble. No self-generation has been observed but the effect of the Lorentz force due to an external magnetic field has been studied (Nataf *et al.* 2006). A similar instrument is being built in Maryland. A sphere of 3 meter in diameter, i.e., much larger than the currently running experiments, is being built with another concentric spherical shell inside. Both spheres can be put into rotation to investigate the effect of global rotation.

5. The VKS experiment

5.1. von Kármán swirling flows

The von Kármán (VK) class of flows consists of flows in which the entrainment is performed by coaxial discs (Zandbergen and Dijkstra 1987). The fluid is enclosed in a cylindrical shell. When the discs are operated in counter-rotation, these flows display various qualities of interest for a potential dynamo: a strong differential rotation and some helicity which are key ingredients for a closed loop induction by ω and α effects. The flow lacks any planar symmetry which is also necessary for the α effect. As shown by measurements of pressure fluctuations, large vorticity concentrations are produced (Fauve *et al.* 1993, Abry *et al.* 1994) which may also act in favour of the amplification of the magnetic field if the classical analogy between vorticity and magnetic field production is to be believed. The choice of VK flows was thus motivated by the hope that the above features will make possible the generation a magnetic field by a strongly turbulent flow.

The induction properties of these flows have been performed at moderate values of R_m up to 7 in Lyon to evidence the various induction steps that may lead to a dynamo (Odier *et al.* 1998, 2000, Volk *et al.* 2006a). With in mind the fact that, in the Riga and Karlsruhe dynamos, the observations fitted very well the prediction from kinematic dynamo computations, an optimisation procedure of the VK flow geometry has been implemented in CEA-Saclay in order to lower the threshold of the dynamo instability and to investigate a potential influence of the high turbulence level on the bifurcation (Marié *et al.* 2003, Ravelet *et al.* 2005). This procedure underlined in particular the importance of the electromagnetic boundary conditions, showing that electrically conducting propellers or possibly fluid motion behind them can increase R_{mc} by a factor 2 (Stefani *et al.* 2006).

5.2. The VKS2 experiment

The VKS acronym stands for “von Kármán Sodium”. The VKS2 experiment is an evolution of a first design, VKS1 (Bourgoin *et al.* 2002, Pétrelis *et al.* 2003) which did not show any dynamo action. The changes compared to the VKS1 design are the implementation of a cooling system and changes in boundary conditions motivated in part by the optimisation procedure discussed above. A sketch of the set-up is displayed in figure 8. The VK flow is generated in the inner cylinder of radius 206 mm and length 524 mm by two counter rotating discs of radius 154 mm and 371 mm apart. The additions to this base flow are a domain of sodium at rest surrounding the VK flow, an annulus in the mid-plane and pure iron discs. The sodium at rest has been shown to lower the threshold in the kinematic simulations using the mean flow. The annulus has been observed to stabilise to some extent the shear layer generated by the counter rotation of the discs. These changes in geometry were not sufficient to develop the dynamo instability and the last change was to use pure iron discs in order to modify the magnetic boundary conditions. In addition to the boundary conditions it also de-couples to some extent the domain in between the discs from the two domains behind the discs, whose flows may not be favourable at least in the kinematic simulations. This last configuration enabled the observation of a dynamo field as shown in figure 9. As the rotation rate of the discs is increased

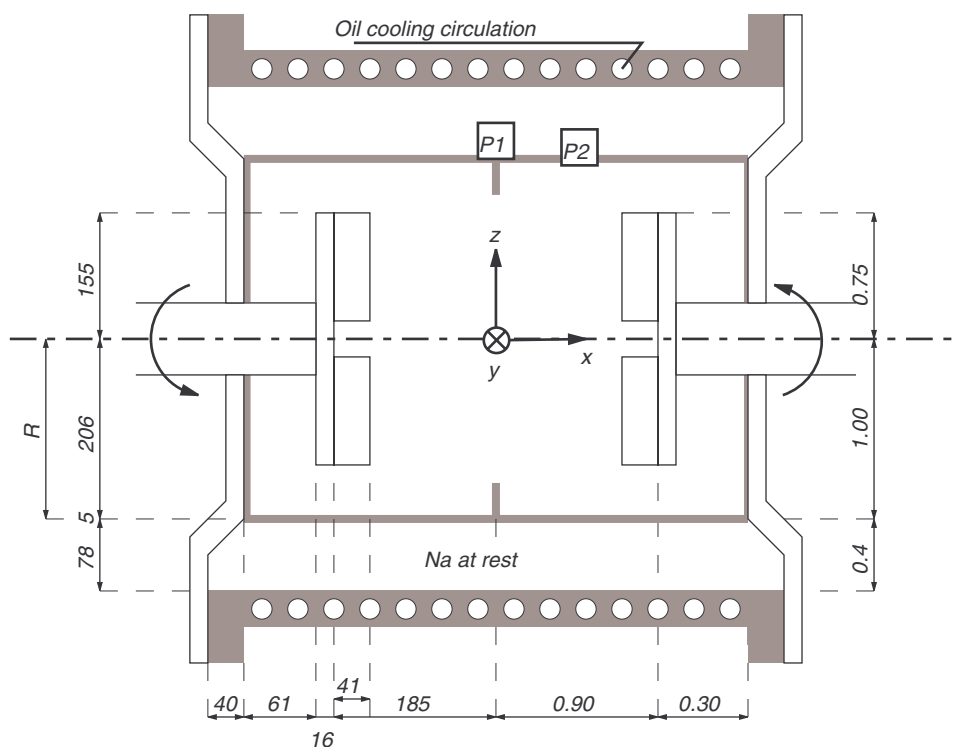


Figure 8. Sketch of the VKS experimental set-up. The inner and outer cylinders are made of copper (in grey) and the other part in stainless steel. The dimensions are given in millimeter on the left half of the drawing and normalised by R on the right half. The 3D Hall probe is located either at point $P1$ in the mid-plane or $P2$. In both cases, the probe is nearly flush with the inner shell. (Figure from Monchaux *et al.* 2007).

from 10 to 22 Hz, one observes at the $P1$ location (see figure 8) the growth of a magnetic field: the azimuthal component acquires a nonzero average value of order 40 Gauss with relatively strong fluctuations. The two other components display small average values but fluctuate with rms values of order 5 gauss. Even though the fluctuation level is much higher than in the Karlsruhe or Riga experiment, we call this dynamo stationary in the sense that it is not displaying any kind of time-periodicity or reversal.

The magnetic Reynolds number in the VKS2 experiment is defined as $R_m = K\mu_0\sigma R^2\Omega$ where R is the radius of the cylinder and Ω the rotation rate of the discs. $K=0.6$ is a numerical coefficient relating ΩR to the maximum velocity in the flow. With this definition the critical magnetic Reynolds number is close to 31 as can be seen from figure 10: the circles correspond to the Lundquist number for VKS2 multiplied by a factor 25.

5.3. Magnetic energy density of fluid dynamos

The dimensionless magnetic energy of the three working dynamos is plotted in figure 10 as a function of the magnetic Reynolds number. The striking feature is that all three

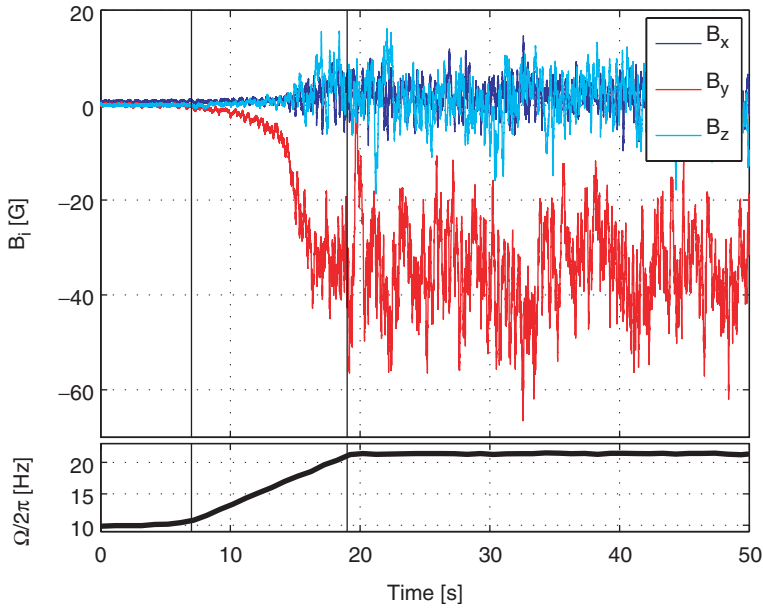


Figure 9. Time recording at position $P1$ (figure 8) of the components of the magnetic field when the rotation frequency $\Omega/2\pi$ is increased as displayed by the ramp below (R_m increases from 19 to 40). (Figure from Monchaux *et al.* 2007).

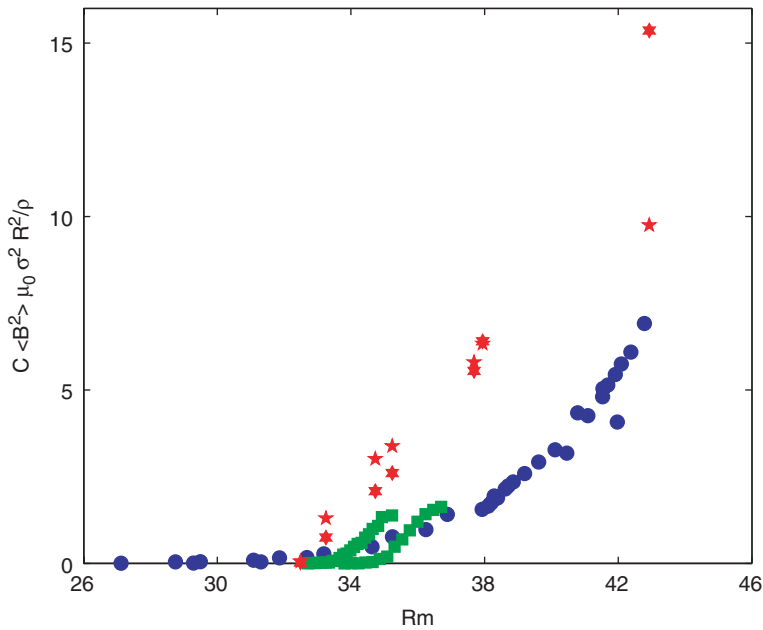


Figure 10. Lundquist number as a function of R_m : Karlsruhe experiment for two ratios of the flow rates (■), Riga experiment (★) and VKS experiment for various working rotation rates and temperatures (●). C is a scaling factor used to display all curves on a single graph. C is one except for the VKS experiment for which $C = 25$. We do not expect to need this factor if measurements are performed in the bulk of the flow instead at the periphery as in Monchaux *et al.* 2007.

dynamoes bifurcate at critical R_m in between 30 and 35. Even though this may be pure coincidence due to a choice of definitions for R_m , it nevertheless means that critical values are really of the same order of magnitude.

The saturation values of the three dynamoes look very similar but again care has to be taken here as the Lundquist number is computed by using only a few localised measurements and not by integrating over the whole volume. This may cause the magnetic energy to be relatively badly estimated depending on the measurement point, even if one expects the scaling properties to be conserved. For instance, the *ad-hoc* factor $C=25$ used for the VKS dynamo can be justified because measurements are performed at the boundary of the flow and thus underestimate the magnetic field intensity.

In any case the laminar scaling would predict magnetic energy 10^5 too small such that for all three dynamoes, the observations are compatible with the turbulent scaling of the saturation of the magnetic energy.

For $R_m > R_{mc}$, the increase of the VKS2 Lundquist number seems of higher order than linear whereas the two other dynamoes show an increase compatible with a linear trend. Whether this behaviour is reminiscent of some anomalous scaling is a difficult question to answer. The fact that the flow displays a much higher turbulence level than the two other dynamoes may be a justification for anomalous scaling (see discussion below) but some care has to be taken in the interpretation of the data. In particular, the presence of the iron discs renders the bifurcation imperfect because of the remanence of the magnetisation in the discs (see discussion below). The apparent nonlinear scaling may be only due to the rather small range of available values for $R_m - R_{mc}$ which may not allow to see the actual scaling. Also because of the imperfection, the apparent R_{mc} may appear lower than the actual one.

6. Further comments and questions about the VKS experiment

6.1. The effect of iron disks

The addition of the iron discs enabled the growth of the dynamo field. Their effect is first to modify the magnetic boundary conditions. For example, when the iron is still in the linear regime with permeability $\mu_0\mu_r$ (i.e., the magnetisation is less than its saturated value), the ferromagnetic metal acts as a shield that prevents the field lines to go across the discs. Field lines are refracted when they penetrate the disc: the normal component of the magnetic field is continuous at the surface but the tangential one is increased by a factor μ_r in the discs. This may de-couple the main flow region in between the discs from the motion of the sodium behind the discs which has been shown by kinematic simulations based on the time averaged flow to increase the threshold of the kinematic dynamo.

The magnetisation vector is also likely to be parallel to the plane of the discs in the same way as an elongated rod is more easily magnetised along its axis. One possibility that agrees with the axial symmetry of the experiment is that the field lines of magnetisation would be loops centred on the cylinder axis. This would act in favour of magnetic field lines with the shape of loops parallel to the discs at least in their vicinity. Such loops with the same orientation as the magnetisation would be stabilised by the presence of the magnetised disc. Next to the disc, the flow is strongly

outwards because of the centrifugal pumping. A material loop of small radius close to the disc would be stretched to a larger radius (see the sketch in figure 12). Thus a magnetic field loop of the same shape would be amplified by the stretching (Fauve and P  tr  lis 2003). The vicinity of the discs acts as an amplifier for the toroidal component of the magnetic field.

As stated before, one consequence of the magnetisation of the discs is that the bifurcation is imperfect. The imperfection is of a different nature than the one in the Karlsruhe experiment. In the latter case, the imperfection was due to the Earth's magnetic field and it was possible to explore the second branch of solutions by imposing an additional external field as shown in figure 3. Here the situation is different: the magnetisation adds an additional contribution to the magnetic field but also the latter can modify the magnetisation. As iron has a low coercive force, the magnetisation can be flipped by a relatively small magnetic field. Let us illustrate this by a simple phenomenological model involving two coupled amplitude equations:

$$\partial_t B = \mu B - B^3 + M, \quad (31)$$

$$\partial_t M = M - M^3 + B. \quad (32)$$

The B variable is the analogue of the amplitude of the magnetic field and displays an instability for positive values of μ without the coupling to the second variable. M is analogous to the magnetisation. The solution $M=0$ is unstable even for $B=0$ as the thermodynamically stable state is the saturated one and iron has a very narrow hysteric cycle and low coercive force. Both variables are positively coupled as the presence of B induces some change of M due to the susceptibility and conversely any nonzero M causes a contribution to B . The nonzero stable solutions are displayed in figure 11 (for $\mu > 1$ other solutions exist but these are not relevant

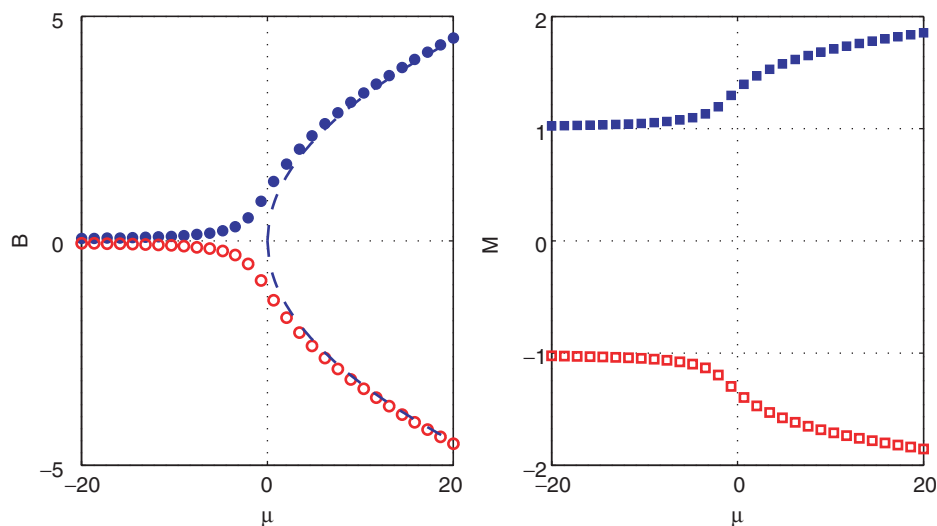


Figure 11. Stable solutions of the phenomenological model (31), (32). On the left is the solution for B and on the right the one for M . Open and full symbols correspond to the same pair of solution (B, M) . The dashed line correspond to the classical bifurcation without coupling $B^2 = \mu$.

for the discussion here). One can see the imperfect bifurcation for B but also that both the positive and negative solutions display the same imperfection due to the coupling with the M variable. Indeed M and B always have the same sign because the low coercive force of iron causes the flip of the magnetisation as soon as the magnetic field changes its sign. This very simple model illustrates the fact that contrary to the Karlsruhe dynamo, both branches of the imperfect bifurcation display the same feature. Applying an external field may force the dynamo to choose one specific branch but the shape would be the same in any case.

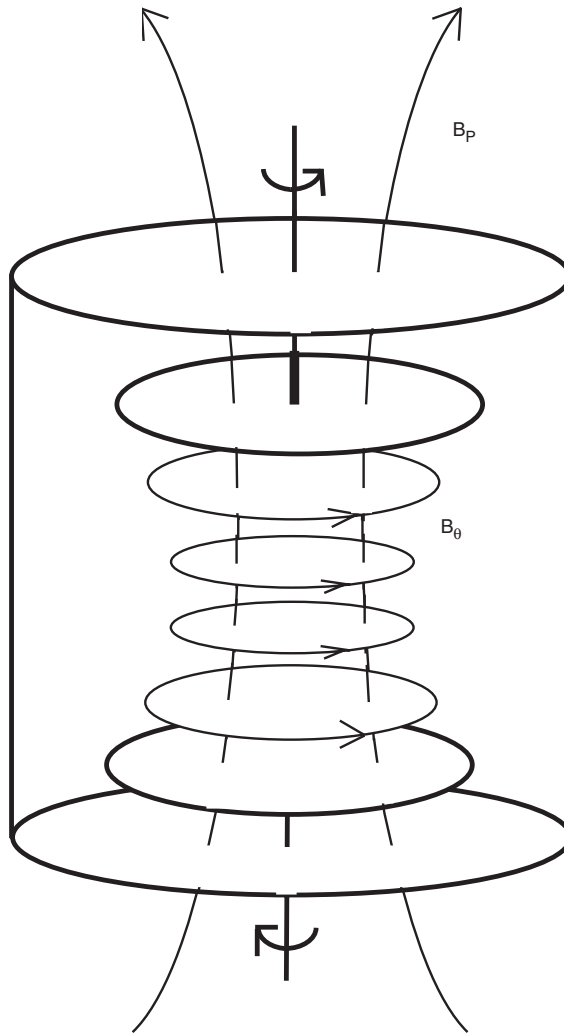


Figure 12. A possible $\alpha - \omega$ mechanism for the VKS experiment using iron discs. Field loops are amplified by the outwards flow close to the discs. The fluid ejected by the discs is also helical due to the differential rotation and can convert the toroidal component B_θ into a poloidal component B_p by α effect. The differential rotation converts also very efficiently the poloidal component into toroidal by ω effect. The relative signs of B_θ and B_p depend on the sign of the helicity.

Note that the $B=0$, $M=0$ state is always linearly unstable. A more realistic description should incorporate space in order to describe magnetic domains and the metastability of the $M=0$ state. However, the aim of this model is just to illustrate that the sign of the imperfection depends on the one of the bifurcating magnetic field and thus is not prescribed by an external broken symmetry.

6.2. A possible dynamo mechanism for the VK flow

Several predictions have been already presented for the VKS dynamo. They are all based on the mean flow alone; the neutral mode has been found dipolar with its axis in the mid-plane between the propellers, i.e. an equatorial dipole (Marié *et al.* 2003, Bourgoïn *et al.* 2004, Ravelet *et al.* 2005, Stefani *et al.* 2006).

The geometry of the experimentally observed magnetic field differs from these predictions. We note that the mean flow being axisymmetric, it cannot generate an axisymmetric magnetic field according to Cowling's theorem. This constraint does not exist for the mean magnetic field generated by the full flow. We give below another possible mechanism that takes into account the helical structure of the radially expelled fluid within two neighbour blades which is averaged out when the mean flow is computed.

The VK flows are very efficient at converting the poloidal components into toroidal one by the ω induction process: axial field lines are twisted by the strong differential rotation and this induces a toroidal component (Odier *et al.* 1998). To get a loop back reaction from toroidal to poloidal, one can invoke an α effect localised close to the discs: the fluid ejected by the discs is strongly helical because of the shear induced by the differential rotation. This is the ingredient required for the α effect to occur. In this way, an axial field can be induced in the cylinder as drawn schematically in figure 12.

If one measures the magnetic field on the cylinder, the poloidal component is most likely weak as the currents that generate it are axisymmetric currents localised in the flow. On the contrary, the toroidal component should be stronger than the poloidal one and more likely to be even stronger when the measurement point is closer to the discs as observed in position *P2*. The observations are compatible with this scenario but a deeper investigation of the dynamo field should be performed to validate it.

In any case, an axisymmetric mean magnetic field cannot be generated by the VKS mean flow because of Cowling's theorem. Thus, according to the definition given in section 4, the VKS experiment with counter-rotating disks generates a turbulent dynamo.

7. Open problems and other possible dynamo experiments

7.1. Anomalous scaling laws for the magnetic energy density?

As said in paragraph 3.2, experimental dynamos operate with liquid metals for which $P_m < 10^{-5}$ and neglecting this dimensionless number in the expression of the energy density leads to the large Re scaling (20). This seems reasonable because the magnetic field is dissipated below the Ohmic scale $L/R_m^{3/4}$ which is much larger than the Kolmogorov scale $L/Re^{3/4}$ at small P_m . It is thus unlikely that the magnetic energy density depends on kinematic viscosity in this limit. However, one should keep in mind that there exist situations where a dimensionless parameter cannot be neglected

even when it becomes much smaller (or larger) than the others. In these infrequent situations, the problem is said to be self-similar of the second kind if the dependence on this parameter is a power law (Barenblatt 1996). This assumption would give an additional dependence P_m^α for the magnetic energy.

We now want to discuss another “nonclassical” effect of the same class that may result from the presence of strong turbulent fluctuations of the velocity field. The magnetic field being forced by many different scales, one may expect a situation similar to critical phenomena for equilibrium phase transitions where large scale thermal fluctuations must be taken into account close to the critical point. This often leads to an “anomalous” behaviour of the order parameter in the vicinity of the transition, where it follows a power law with a critical exponent that differs from the mean field prediction. Although thermal fluctuations may in principle also affect the amplitude of neutral modes in the vicinity of instability thresholds, it has been shown that this anomalous behaviour, if it exists, would be limited to a very small range and thus not detectable for most hydrodynamic instabilities (Hohenberg and Swift 1992). Various hydrodynamical instabilities have been studied using liquid crystals (Rehberg *et al.* 1991) or in the vicinity of the liquid–vapour critical point (Fauve *et al.* 1992, Oh and Ahlers 2003) in order to try to enhance the effect of thermal fluctuations. Although some effects have been observed, to the best of our knowledge, no anomalous dependence of the amplitude of unstable modes above threshold has been reported. Only mean field exponents, i.e., rational power laws given by simple symmetry arguments have been measured so far. For a supercritical instability, this assumption led to (19), i.e., $f(R_m, P_m) \propto \sqrt{(R_m - R_{mc})}$, thus a mean field exponent 1/2.

As said above, in phase transitions departure from mean-field theory occurs when the thermal fluctuations cannot be neglected. This is expressed by the Ginzburg criterion that compares the amplitude of the order parameter predicted by mean field theory to the effect of thermal fluctuations (Ginzburg 1960). Using a similar criterion, but taking into account the kinetic energy E_F of turbulent velocity fluctuations instead of kT , would give an interval range above the dynamo threshold where an anomalous scaling can be expected. It may be wrong to compare macroscopic turbulent fluctuations to temperature and estimating the number of relevant modes is difficult. However, if we assume that the mean field undergoes a pitchfork bifurcation and that the dependence of its amplitude in space involves a Laplacian to leading order, dimensional arguments lead to

$$\frac{R_m - R_{mc}}{R_{mc}} < \left[\frac{\mu_0 E_F}{B_0^2 \xi_0^3} \right]^2, \quad (33)$$

where B_0 is the pre-factor of the magnetic field above threshold in mean field theory and ξ_0 the one of its correlation length. Inserting the large Re scaling (19) for B_0 , and taking into account that fluctuations are of the same order of magnitude as the mean flow, we obtain

$$\frac{R_m - R_{mc}}{R_{mc}} < \left[\frac{L}{\xi_0} \right]^6, \quad (34)$$

that can be of order one even if $\xi_0 \simeq L$. We thus expect that a critical region in R_m with an anomalous scaling of the mean amplitude of the magnetic field can be easily observed. This can be understood since the energy of the fluctuations is significant compared to the one needed to reverse the magnetic field slightly above the dynamo threshold.

The above estimate of the range in $R_m - R_{mc}$ where an anomalous behaviour can be expected depends of course on the nature of the bifurcation. For instance, if an equatorial mean field were generated, we expect the effect of fluctuations to be stronger than for an axisymmetric mean field because the orientation of the dipole can easily rotate under the influence of fluctuations. This is reminiscent of the sensitivity of critical behaviour on the broken symmetry of the ordered phase: fluctuations have a deeper effect when a continuous symmetry is broken. For instance the ordered phase is destroyed by the thermal fluctuations for a two dimensional XY spin model because the ordered phase breaks the axisymmetry of the problem. On the contrary, for a two dimensional Ising model, the ordered phase is axisymmetric and is not destroyed by the fluctuations (Goldenfeld 1992).

We can argue that velocity fluctuations act in a multiplicative way whereas thermal fluctuations in phase transitions are additive. We note that in the presence of Earth's magnetic field, velocity fluctuations also involve additive forcing. In addition, even in the absence of any ambient field, the small scale fluctuations of the magnetic field are forced by an additive term resulting from the interaction between the small scale fluctuations of the velocity and the mean magnetic field generated by the dynamo. Differences from the mean field behaviour are expected as soon as the fluctuations of the magnetic field are of the same order as its mean value. Together with the hypothesis of self similarity of the second kind, the magnetic energy would then behave as

$$\left\langle \frac{B^2}{\mu_0} \right\rangle = \rho V^2 P_m^\alpha (R_m - R_{mc})^\beta. \quad (35)$$

with $\beta \neq 1/2$. The results of the VKS experiment cannot presently be used to test this type of behaviour because of the imperfection due to the iron discs close to threshold. Thus, it is necessary to increase its maximum magnetic Reynolds number or to find a more efficient flow in order to obtain a turbulent dynamo without using iron discs.

7.2. An optimised α - ω dynamo?

If one is to believe the induction scenario proposed above, then it may be possible to improve further the efficiency of the effects possibly involved in the VKS dynamo. We propose the set-up described in figure 13: a VK flow is driven by two coaxial discs with a narrow gap. A very strong shear is thus created between these two impellers. The discs are fitted with blades resulting in a strong radial outward flow that expels the fluid. The discs centres are hollowed: the fluid expelled radially loops back into the gap by these openings. The radial velocity and the azimuthal shear result in a strongly helical flow. Therefore the flow displays two ingredients described above: a strong helicity and a strong differential rotation that drive respectively an α effect and an ω effect. With this modified set-up, one avoids the central region of the

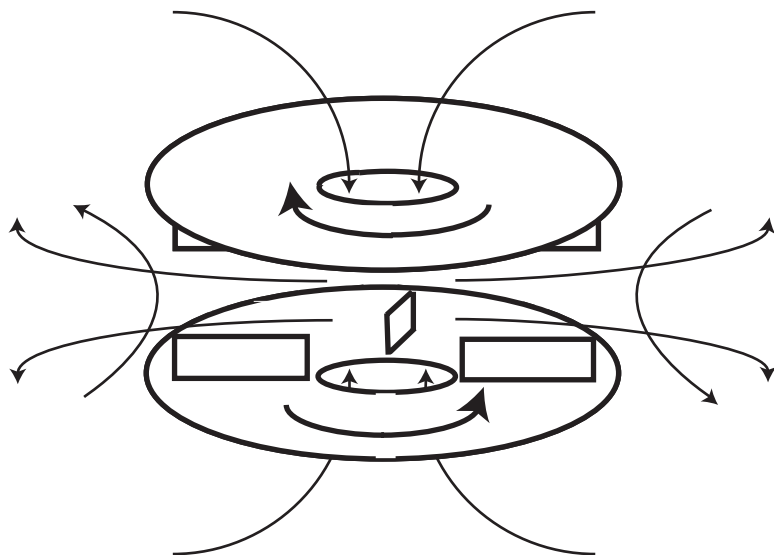


Figure 13. An optimised α - ω dynamo experiment.

VKS experiment where the flow is radially inbound which tends to dampen the toroidal component of the flow. The expected unstable mode is qualitatively similar to the one described above for VKS, roughly axisymmetric and made of two parts: a poloidal field with same axis as the discs and an azimuthal field. The converging region is farther from the amplification region and is partially shielded if iron discs are used so that one expects this flow to be more efficient and to possibly lead to a lower critical magnetic Reynolds number. If the gain of efficiency due to the absence of radially inward flow in the mid-plane is large enough, one may also observe self-generation without using iron discs.

7.3. Non axisymmetric dynamos

All currently working dynamos are based on axisymmetric flows. The time-averaged velocity field of the Riga and VKS dynamos are invariant by rotation around the axis of their propellers. For the large scale magnetic field generated in the Karlsruhe experiment, the α -effect created by the cellular flow is invariant by rotation around the axial direction of the flow.

Symmetries usually do not favour dynamo action. There is no α -effect if the flow displays any planar symmetry. Anti-dynamo theorems are related to the symmetries of the flow or of the magnetic field.

A non-axisymmetric flow can be generated by driving a fluid with a set of propellers located at positions not aligned along their axis of rotation. A gallium-experiment based on such flow is currently studied at ENS-Paris (Berhanu *et al.* 2007). It is driven by two pairs of propellers. Depending on their pitch and on the sign of their angular velocity, different flows that result from interacting vortices generated by the propellers are observed. Such flows relieve the constraint of axisymmetry and may be efficient for induction or dynamo action.

In addition, the large scale vortices interact, thus leading to fluctuations of the flow at low frequencies. This is probably important in order to generate dynamos that are strongly affected by the flow fluctuations. Low frequency fluctuations are indeed required in order to have on–off intermittency in low dimensional dynamical systems (Aumaître *et al.* 2005). Similarly, these fluctuations might favour the occurrence of anomalous exponents for the magnetic energy of turbulent dynamos.

Finally we point out that a set of vortices generally leads to chaotic Lagrangian trajectories. This is an important ingredient for fast dynamo action (Childress and Gilbert 1995). Although there is no hope to reach very large values of Rm in an experimental dynamo, studying the growth rate of the magnetic field at moderate Rm in a flow displaying Lagrangian chaos at large scale can provide useful information.

8. Concluding remarks

The dynamo threshold and the geometry of the generated magnetic field in the Karlsruhe and Riga experiments were correctly predicted by taking into account the mean flow alone. This observation is supported by an argument showing that due to the low level of fluctuations, the shift in threshold has to be of order two at least in the amplitude of turbulent fluctuations. On the contrary, the geometry of the magnetic field generated in the VKS experiment cannot be generated by the mean flow alone. Large scale turbulent fluctuations are of the same order of magnitude as the mean flow because the flow is much less constrained. Although this needs to be confirmed with a detailed experimental study, we suggest a dynamo mechanism based on a α – ω process that implies a non stationary part of the VK flow, suggesting that the observed dynamo is turbulent (in the meaning used in this article).

The three fluid dynamo experiments show that the magnetic energy density in the saturated regime above threshold is such that the Lundquist number is of the order of the distance to criticality. This results from the large value of the kinetic Reynolds number.

The Karlsruhe and Riga experiments as well as the VKS experiment with propellers in exact counter-rotation, have not displayed secondary bifurcations generating large scale dynamics of the magnetic field. However, it should be noted that for propellers driven at different rotation frequencies, a great variety of dynamical regimes (stationary, oscillatory, intermittent) as well as reversals of the magnetic field have been observed in the VKS experiment (Berhanu *et al.* 2007). It is likely that this results from the presence of competing instability modes that can be also observed in less turbulent dynamos by tuning two different control parameters. The effect of the fully turbulent character of the VKS2 experiment on these dynamical regimes deserves new experiments.

Acknowledgements

We acknowledge Dr F. Stefani and Dr Robert Stieglitz for providing data and figures related to the Riga and Karlsruhe experiments (figures 1–7, 10). We thank all the participants of the VKS collaboration with whom experiments related to figures 8–10 have been performed.

References

- Abry, P., Fauve, S., Flandrin, P. and Laroche, C., Analysis of pressure fluctuations in swirling turbulent flows. *J. Physique II*, 1994, **4**, 725–733.
- Aumaitre, S., Pétrélis, F. and Mallick, K., Low-frequency noise controls on–off intermittency of bifurcating systems. *Phys. Rev. Lett.*, 2005, **95**, 064101.
- Aumaitre, S., Mallick, K., Petrelis, F., Effects of the low frequencies of noise on on-off intermittency. *J. Statis. Phys.*, 2006, **123**, 909–927.
- Barenblatt, G.I., *Scaling, Self-similarity, and Intermediate Asymptotics*, 1996 (Cambridge University Press: Cambridge).
- Bassom, A.P. and Gilbert, A.D., Nonlinear equilibration of a dynamo in a smooth helical flow. *J. Fluid Mech.*, 1997, **343**, 375–406.
- Berhanu, M., Mordant, N. and Fauve, S., Ecoulement turbulent dans un cylindre: haut nombre de Reynolds et fluctuations à basse fréquence (Rencontres du non linéaire, 2007).
- Berhanu, M., Monchaux, R., Fauve, S., Mordant, N., Pétrélis, F., Chiffaudel, A., Daviaud, F., Dubrulle, B., Marié, L., Ravelet, F., Bourgoin, M., Odier, Ph., Pinton, J.-F., Volk, R., Magnetic field reversals in an experimental turbulent dynamo. *Europhys. Lett.*, 2007, **77**, 59001.
- Berthet, R., Petrossian, A., Residori, S., Roman, B. and Fauve, S., Effect of multiplicative noise on parametric instabilities. *Physica D*, 2003 **174**, 84–99.
- Bourgoin, M., Odier, P., Pinton, J.F. and Ricard, Y., An iterative study of time independent induction effects in magnetohydrodynamics. *Phys. Fluids*, 2004, **16**, 2529–2547.
- Bourgoin, M., Marié, L., Pétrélis, F., Gasquet, C., Guigon, A., Luciani, J.B., Moulin, M., Namer, F., Burgete, J., Chiffaudel, A., Daviaud, F., Fauve, S., Odier, P. and Pinton, J.F., Magnetohydrodynamics measurements in the von Kármán sodium experiment. *Phys. Fluids*, 2002, **14**, 3046–3058.
- Busse, F.H., A model of the geodynamo. *Geophys. J. R. Astr. Soc.*, 1975, **42**, 437–459.
- Busse, F.H., Müller, U., Stieglitz, R. and Tilgner, A., A two-scale homogeneous dynamo, and extended analytical model and an experimental demonstration under development. *Magnetohydrodynamics*, 1996, **32**, 235–248.
- Cattaneo, F. and Hughes, D.W., Dynamo action in a rotating convective layer. *J. Fluid Mech.*, 2006, **553**, 401–418.
- Childress, S. and Gilbert, A.D., *Stretch, Twist, Fold: The fast dynamo*, 1995 (Springer Verlag: Berlin, Heidelberg).
- Childress, S. and Soward, A.M., Convection driven hydromagnetic dynamo. *Phys. Rev. Lett.*, 1972, **29**, 837–839.
- Dudley, M.L. and James, R.W., Time-dependent kinematic dynamos with stationary flows. *Proc. R. Soc. London A*, 1989, **425**, 407–429.
- Fauve, S. and Pétrélis, F., The dynamo effect. In *Peyresq Lectures on Nonlinear Phenomena*, edited by J.-A. Sepulchre, Vol. II, pp. 1–64, 2003 (World Scientific: Singapore).
- Fauve, S. and Lathrop, D.P., Laboratory experiments on liquid metal dynamos and liquid metal MHD turbulence. In *Fluid Dynamics and Dynamos in Astrophysics and Geophysics*, edited by A. Soward *et al.*, pp. 393–425, 2005 (CRC Press: USA).
- Fauve, S. and Pétrélis, F., Scaling laws of turbulent dynamos. *C. R. Physique*, 2007, **8**, 87–92.
- Fauve, S., Laroche, C. and Castaing, B., Pressure fluctuations in swirling turbulent flows. *J. Physique II*, 1993, **3**, 271–278.
- Fauve, S., Kumar, K., Laroche, C., Beysens, D. and Garrabos, Y., Parametric instability of a liquid-vapor interface close to the critical point. *Phys. Rev. Lett.*, 1992, **68**, 3160.
- Forest, C.B., Bayliss, R.A., Kendrick, R.D., Nornberg, M.D., O’Connell, R. and Spence, E.J., Hydrodynamic and numerical modeling of a spherical homogeneous dynamo experiment. *Magnetohydrodynamics*, 2002, **38**, 107–120.
- Frick, P., Denisov, S., Khripchenko, S., Noskov, V., Sokoloff, D. and Stepanov, R., A nonstationary dynamo experiment in a braked torus. In *Dynamo and Dynamics, a Mathematical Challenge*, edited by P. Chossat *et al.*, pp. 1–8, 2001 (Kluwer Academic Publishers: Dordrecht).
- Gailitis, A., Lielausis, O., Platācis, E.A., Gerbeth, G., Stefani, F., Laboratory experiments on hydromagnetic dynamos. *Rev. Mod. Phys.*, 2002, **74**, 973990.
- Gailitis, A., Lielausis, O., Platācis, E., Gerbeth, G., Stefani, F., The Riga dynamo experiment. *Surveys in Geophysics*, 2003, **24**, 247–267.
- Gailitis, A., Lielausis, O., Platācis, E., Dement’ev, S., Cifersons, A., Gerbeth, G., Gundrum, T., Stefani, F., Christen, M. and Will, G., Magnetic field saturation in the Riga dynamo experiment. *Phys. Rev. Lett.*, 2001, **86**, 3024–3027.
- Galloway, D.J. and Proctor, M.R.E., Numerical calculations of fast dynamos in smooth velocity fields with realistic diffusion. *Nature (London)*, 1992, **356**, 691–693.

- Gans, R.F., On hydromagnetic precession in a cylinder. *J. Fluid Mech.*, 1970, **45**, 111–130.
- Gilbert, A.D. and Sulem, P.L., On inverse cascades in alpha effect dynamos. *GAFD*, 1990, **51**, 243–261.
- Ginzburg, V.L., Some remarks on phase transitions of the second kind and the microscopic theory of ferroelectric materials. *Soviet Phys. Solid State*, 1960, **2**, 1824–1834.
- Goldenfeld, N., *Lectures on Phase Transitions and the Renormalization Group*, 1985 (Addison-Wesley: USA).
- Hohenberg, P.C. and Swift, J.B., Effects of additive noise at the onset of Rayleigh-Bénard convection. *Phys. Rev. A*, 1992, **46**, 4773–4785.
- Hoyng, P., Helicity fluctuations in mean field theory: an explanation for the variability of the solar cycle? *Astron. Astrophys.*, 1993, **272**, 321–339.
- Hughes, D.W. and Cattaneo, F., The α -effect in rotating convection: size matters, submitted to *J. Fluid Mech.*, 2007.
- Iroshnikov, P.S., Turbulence of a conducting fluid in a strong magnetic field. *Soviet Astron.*, 1963, **7**, 566–571.
- John, T., Stannarius, R. and Behn, U., On-off intermittency in stochastically driven electrohydrodynamic convection in nematics. *Phys. Rev. Lett.*, 1999, **83**, 749–752.
- Kabashima, S., Kogure, S., Kawakubo, T. and Okada, T., Oscillatory-to-nonoscillatory transition due to external noise in a parametric oscillator. *J. Appl. Phys.*, 1979, **50**, 6296–6302.
- Knobloch, E., Private communication (2007).
- Kraichnan, R.H., Inertial-range spectrum of hydromagnetic turbulence. *Phys. Fluids*, **8**, 1965, 1385–1387.
- Krause, F. and Rädler, K.-H., *Mean Field Magnetohydrodynamics and Dynamo Theory*, 1980 (Pergamon Press: New-York).
- Larmor, J., How could a rotating body such as the sun become a magnet?, Rep. 87th Meeting Brit. Assoc. Adv. Sci., Bornemouth, Sept. 9–13, 1919, pp. 159–160, 1919 (John Murray: London).
- Laval, J.P., Blaineau, P., Leprovost, N., Dubrulle, B. and Daviaud, F., Influence of turbulence on the dynamo threshold. *Phys. Rev. Lett.*, 2006, **96**, 204503.
- Lehnert, B., An experiment on axisymmetric flow of liquid sodium in a magnetic field. *Arkiv för Fysik*, 1957, **13**, 109–116.
- Léorat, J., Lallemand, P., Guermond, J.L. and Plunian, F., Dynamo action, between numerical experiments and liquid sodium devices. In *Dynamo and Dynamics, a Mathematical Challenge*, edited by P. Chossat *et al.*, pp. 25–33, 2001 (Kluwer Academic Publishers: Dordrecht).
- Lücke, M. and Schank, F., Response to parametric modulation near an instability. *Phys. Rev. Lett.*, 1985, **54**, 1465–1468.
- Malkus, W.V.R., Precession of the Earth as the cause of geomagnetism. *Science*, 1968, **160**, 259–264.
- Marié, L., Burguete, J., Daviaud, F. and Léorat, J., Numerical study of homogeneous dynamo based on experimental von Kármán type flows. *Eur. Phys. J. B*, 2003, **33**, 469–485.
- Moffatt, H.K., The amplification of a weak applied magnetic field by turbulence in fluids of moderate conductivity, *J. Fluid Mech.*, 1961, **11**, 625–635.
- Moffatt, H.K., *Magnetic Field Generation in Electrically Conducting Fluids*, 1978 (Cambridge University Press: Cambridge).
- Monchaux, R., Berhanu, M., Bourgoin, M., Moulin, M., Odier, Ph., Pinton, J.-F., Volk, R., Fauve, S., Mordant, N., Pétrélis, F., Chiffaudel, A., Daviaud, F., Dubrulle, B., Gasquet, C. and Marié, L., Generation of magnetic field by dynamo action in a turbulent flow of liquid sodium. *Phys. Rev. Lett.*, 2007, **98**, 044502.
- Müller, U., Stieglitz, R. and Busse, F.H., On the sensitivity of dynamo action to the system's magnetic diffusivity, *Phys. Fluids*, 2004, **16**, L87–90.
- Nataf, H.C., Alboussière, T., Brito, D., Cardin, P., Gagnière, N., Jault, D., Masson, J.-P. and Schmitt, D., Experimental study of super-rotation in a magnetostrophic spherical Couette flow. *GAFD*, 2006, **100**, 281–298.
- Nornberg, M.D., Spence, E.J., Kendrick, R.D., Jacobson, C.M. and Forest, C.B., Intermittent magnetic field excitation by a turbulent flow of liquid sodium. *Phys. Rev. Lett.*, 2006, **97**, 044503.
- Núñez, A., Pétrélis, F. and Fauve, S., Saturation of a Ponomarenko type fluid dynamo. In *Dynamo and Dynamics, a Mathematical Challenge*, edited by P. Chossat *et al.*, pp. 67–74, 2001 (Kluwer Academic Publishers: Dordrecht).
- Odier, P., Pinton, J.F. and Fauve, S., Advection of a magnetic field by a turbulent swirling flow. *Phys. Rev. E*, 1998, **58**, 7397–7401.
- Odier, P., Pinton, J.-F. and Fauve, S., Magnetic induction by coherent vortex motion. *Eur. Phys. J. B*, 2000, **16**, 373–378.
- Oh, J. and Ahlers, G., Thermal noise effect on the transition to Rayleigh-Bénard convection. *Phys. Rev. Lett.*, 2003, **91**, 094501.
- Parker, E.N., The occasional reversal of the geomagnetic field. *Astrophys. J.*, 1969, **158**, 815–827; Peffley, N.L., Cawthorne, A.B. and Lathrop, D.P., Toward a self-generating magnetic dynamo: the role of turbulence. *Phys. Rev. E*, 2000, **61**, 5287–5294.

- Pétrélis, F., Etude des mécanismes d'instabilité et de saturation du champ magnétique. PhD thesis, 2002 (Université Paris 6).
- Pétrélis, F. and Fauve, S., Saturation of the magnetic field above the dynamo threshold. *Eur. Phys. J. B*, 2001, **22**, 273–276.
- Pétrélis, F. and Aumaitre, S., Intermittency at the edge of a stochastically inhibited pattern-forming instability. *Eur. Phys. J. B*, 2003, **34**, 281–284.
- Pétrélis, F. and Aumaitre, S., Modification of instability processes by multiplicative noises. *Euro. Phys. J. B*, 2006, **51**, 357–362.
- Pétrélis, F. and Fauve, S., Inhibition of the dynamo effect by phase fluctuations. *Europhys. Lett.*, 2006, **76**, 602–608.
- Pétrélis, F., Aumaitre, S. and Fauve, S., Effects of phase noise on the Faraday instability. *Phys. Rev. Lett.*, 2005, **94**, 070603.
- Pétrélis, F., Bourgoin, M., Marié, L., Burgete, J., Chiffaudel, A., Daviaud, F., Fauve, S., Odier, P. and Pinton, J.F., Nonlinear magnetic induction by helical motion in a liquid sodium turbulent flow. *Phys. Rev. Lett.*, 2003, **90**, 174501.
- Platt, N., Spiegel, E.A. and Tresser, C., On-off intermittency: a mechanism for bursting. *Phys. Rev. Lett.*, 1993, **70**, 279–282, and references therein.
- Platt, N., Hammel, S. and Heagy, J., Effect of additive noise on on-off intermittency. *Phys. Rev. Lett.*, 1994, **72**, 3498–3501.
- Ponomarenko, Yu.B., Theory of the hydromagnetic generator. *J. Appl. Mech. Tech. Phys.*, 1973, **14**, 775–778.
- Ponty, Y., Mininni, P.D., Montgomery, D.C., Pinton, J.-F., Politano, H. and Pouquet, A., Numerical study of dynamo action at low magnetic Prandtl numbers. *Phys. Rev. Lett.*, 2005, **94**, 164502; Ponty, Y., Mininni, P., Pinton, J.F., Politano, H. and Pouquet, A., Dynamo action at low magnetic Prandtl numbers: mean flow vs. fully turbulent motion (arXivphysics/0601105), to be published in *New J. Phys.*, 2007.
- Rädler, K.-H., Apstein, E., Rheinhardt, M. and Schüler, M., The Karlsruhe dynamo experiment. A mean field approach. *Studia Geophys. Geod.*, 1998, **42**, 224–231.
- Ravelet, F., Chiffaudel, A., Daviaud, F. and Léorat, J., Toward an experimental von Kármán dynamo: numerical studies for an optimized design. *Phys. Fluids*, 2005, **17**, 117104.
- Rehberg, I., Rasenat, S., de la Torre Juárez, M., Schöpf, W., Hörner, F., Ahlers, G. and Brand, H.R., Thermally induced hydrodynamic fluctuations below the onset of electroconvection. *Phys. Rev. Lett.*, 1991, **67**, 596–599.
- Reighard, A.B. and Brown, M.R., Turbulent conductivity measurements in a spherical liquid sodium flow. *Phys. Rev. Lett.*, 2001, **86**, 2794–2797.
- Residori, S., Berthet, R., Roman, B. and Fauve, S., Noise induced bistability of parametric surface waves. *Phys. Rev. Lett.*, 2001, **88**, 024502.
- Roberts, G.O., Dynamo action of fluid motions with two-dimensional periodicity. *Phil. Trans. Roy. Soc. London A*, 1972, **271**, 411–454.
- Roberts, P.H., Future of geodynamo theory. *GAFD*, 1988, **44**, 3–31, and references therein.
- Roberts, P.H., Fundamentals of dynamo theory. In *Lectures on Solar and Planetary Dynamos*, pp. 1–57, edited by M.R.E. Proctor and A.D. Gilbert, 1994 (Cambridge University Press: Cambridge).
- Ruzmaikin, A.A. and Shukurov, A.M., Spectrum of the galactic magnetic fields. *Astrophys. Space Sci.*, 1982, **82**, 397–407.
- Soward, A.M., A convection-driven dynamo: I. The weak field case. *Phil. Trans. R. Soc. Lond.*, 1974, **A 275**, 611–646.
- Spence, E.J., Nornberg, M.D., Jacobson, C.M., Kendrick, R.D. and Forest, C.B., Observation of a turbulence-induced large scale magnetic field. *Phys. Rev. Lett.*, 2006, **96**, 055002.
- Stefani, F., Xu, M., Gerbeth, G., Ravelet, F., Chiffaudel, A., Daviaud, F. and Léorat, J., Ambivalent effects of added layers on steady kinematic dynamos in cylindrical geometry: application to the VKS experiment. *Eur. J. Mech. B*, 2006, **25**, 894.
- Stieglitz, R. and Müller, U., Experimental demonstration of a homogeneous two-scale dynamo. *Phys. Fluids*, 2001, **13**, 561–564.
- Stieglitz, R. and Müller, U., Experimental demonstration of a homogeneous two-scale dynamo. *Magnetohydrodynamics*, 2002, **38**, 27–34.
- Stratonovich, R.L., *Topics in the Theory of Random Noise*, 1963 (Gordon and Breach: London).
- Sweet, D., Ott, E., Finn, J., Antonsen, T.M. and Lathrop, D., Blowout bifurcations and the onset of magnetic activity in turbulent dynamos. *Phys. Rev. E*, 2001, **63**, 066211, 1–4.
- Tilgner, A. and Busse, F.H., Saturation mechanism of a model of the Karlsruhe dynamo. In *Dynamo and Dynamics, a Mathematical Challenge*, edited by P. Chossat et al., pp. 109–116, 2001 (Kluwer Academic Publishers: Dordrecht).
- Verma, M.K., Statistical theory of magnetohydrodynamic turbulence: recent results. *Phys. Rep.*, 2004, **401**, 229–380.

- Volk, R., Odier, P. and Pinton, J.-F., Fluctuation of magnetic induction in von Kármán swirling flows. *Phys. Fluids*, 2006a, **18**, 085105.
- Volk, R., Ravelet, F., Monchaud, R., Berhanu, M., Chiffaudel, A., Daviaud, F., Odier, P., Pinton, J.-F., Fauve, S., Mordant, N. and Pétrélis, F., Transport of magnetic field by a turbulent flow of liquid sodium. *Phys. Rev. Lett.*, 2006b, **97**, 074501.
- Zandbergen, P.J. and Dijkstra, D., von Kármán swirling flows. *Annu. Rev. Fluid Mech.*, **19**, 1987, 465–491.
- Zeldovich, Ya.B., Ruzmaikin, A.A. and Sokoloff, D.D., *Magnetic Fields in Astrophysics*, 1983 (Gordon and Breach: New York).